ENGINEERING RESEARCH INSTITUTE
UNIVERSITY OF MICHIGAN
ANN ARBOR

THEORETICAL STUDY, DESIGN AND CONSTRUCTION OF C-W MAGNETRONS FOR FREQUENCY MODULATION

QUARTERLY PROGRESS REPORT NO. 2

Period Covering March 1, 1950, to June 1, 1950
Electron Tube Laboratory
Department of Electrical Engineering

BY

H. W. WELCH, JR.

J. R. BLACK

G. R. BREWER

J. S. NEEDLE

W. PETERSON

Approved By: W. G. Dow
G. Hok

Project M762

CONTRACT NO. W-36-039 sc-35561
SIGNAL CORPS, DEPARTMENT OF THE ARMY
DEPARTMENT OF ARMY PROJECT NO. 399-13-022
SIGNAL CORPS PROJECT NO. 112B-0

July, 1950

TABLE OF CONTENTS

1. OBJECTIVES FOR THE PERIOD 1

2. LOW Q OPERATION OF MAGNETRONS 3

3. FREQUENCY PUSHING 5

4. MAXIMUM CURRENT BOUNDARY--General 25

5. SPACE CHARGE LIMITED CURRENT LIMITATION IN THE OSCILLATING MAGNETRON 28

6. TEMPERATURE LIMITED OPERATION 37

7. LOW POWER MAGNETRON FOR LOW Q OPERATION 45

8. EXPERIMENT ON D.C. MAGNETRON 48

9. R-F PROPERTIES OF MAGNETRON SPACE CHARGE 55

A. Propagation of electromagnetic waves in a magnetron space charge-- theoretical analysis 55

B. Experimental investigation 71

10. CONSTRUCTION AND TESTING OF MAGNETRONS 77

11. CONCLUSIONS 84

12. WORK IN PROSPECT 86

DISTRIBUTION LIST 87

PERSONNEL

Scientific and Engineering Personnel		* Time worked in man-months.
W. G. Dow	Prof. of Electrical Engineering	Supervisor
H. W. Welch	Research Physicist	2.52
J. R. Black	Research Engineer	2.98
G. Hok	Research Engineer	.20
H. A. Martens	Research Engineer	1.30
J. S. Needle	Research Engineer	.28
G. R. Brewer	Research Associate	2.82
H. W. Batten	Student Assistant	.86
W. W. Peteron	Student Assistant	1.38

Service Personnel		
V. R. Burris	Machine Shop Foreman	1.21
R. F. Steiner	Assembly Technician	2.96
J. W. VanNatter	Assembly Technician	2.93
J. Mossar	Technician	1.14
M. J. Walker	Stenographer	1.01
S. Spiegelman	Stenographer	.86
D. L. McCormick T. G. Keith E. A. Kayser R. F. Denning	Laboratory Machinists	5.44
Miscellaneous Services		.53

* Time worked is figured on the basis of 172 hours per month.

MAJOR REPORTS ISSUED TO DATE

Contract No. W-36-039 sc-32245. Subject: Theoretical Study, Design and Construction of C-W Magnetrons for Frequency Modulation.

Technical Report No. 1 --

H. W. Welch, Jr. "Space-Charge Effects and Frequency Characteristics of C-W Magnetrons Relative to the Problem of Frequency Modulation", November 15, 1948.

Technical Report No. 2 --

H. W. Welch, Jr., G. R. Brewer. "Operation of Interdigital Magnetrons in the Zero Order Mode", May 23, 1949.

Technical Report No. 3 --

H. W. Welch, Jr., J. R. Black, G. R. Brewer, G. Hok. "Final Report", May 27, 1949.

Contract No. W-36-039 sc-35561. Subject: Theoretical Study, Design and Construction of C-W Magnetrons for Frequency Modulation.

Interim Report --

H. W. Welch, Jr., J. R. Black, G. R. Brewer. December 15, 1949.

Quarterly Report No. 1 --

H. W. Welch, Jr., J. R. Black, G. R. Brewer, G. Hok, April, 1950.

LIST OF FIGURES

Fig. 3.1 Pictorial Representation of Space Charge Within Interaction Space.

Fig. 3.2 Equivalent Circuit for Oscillating Magnetron.

Fig. 3.3 Change of Magnetron Resonant Wavelength with Plate Voltage.

Fig. 3.4 Parameters Involved in Equation 3.1 Applying to Circuit of Fig. 3.2.

Fig. 3.5 Load Diagram Model 3 No. 8.

Fig. 3.6 Comparison of Pushing Data and Theory.

Fig. 3.7 Logarithmic Plot of Data from Table 3.2.

Fig. 3.8 Generator Current (I_g) Calculated from Equation 3.9 Compared with I_b and Phase Angle ϕ as a Function of Load Power.

Fig. 5.1 Ratio of Space Charge Limited Current of Magnetic Diode to that of Ordinary Diode (i.e. Allis Current to Langmuir Current) as a Function of r/r_c.

Fig. 5.2 Space Charge Limited Current in Oscillating Magnetron from Equations 5.1 and 5.2.

Fig. 5.3 Space Charge Limited Current in Oscillating Magnetron from Equations 5.1 and 5.2

Fig. 6.1 Effect of Emission on Maximum Current Boundary--Raytheon Data.

Fig. 6.2 Effects of Loading on Maximum Current Boundary--Raytheon Data.

Fig. 6.3 Effect of Magnetic Field on Maximum Current Boundary--Raytheon Data.

Fig. 6.4 Comparison of Space Charge Free and Magnetron Space Charge Condition.

Fig. 7.1 Sketch of Low Power Magnetron for Use in External Tunable Cavity.

Fig. 8.1 Potential Distribution in Plane Diodes.

Fig. 8.2 Space Charge Distribution in Plane Diodes.

Fig. 9.1 Coordinate System and Field Vectors of Plane Magnetron.

Fig. 9.2 ε_{eff} for Plane Magnetron.

Fig. 9.3a Index of Refraction of Plane Magnetron.

Fig. 9.3b Index of Refraction of Plane Magnetron.

Fig. 9.4 Coordinate System and Field Vectors of Cylindrical Magnetron.

Fig. 9.5 ε_{eff} for Cylindrical Magnetron.

Fig. 9.6 ε_{eff} for Cylindrical Magnetron.

Fig. 9.7 10 cm Magnetron Diode (Experimental) Model 3.

Fig. 9.8 TE_{011} Resonant Cavity for Space Charge Study.

Fig. 9.9 Section of Field Map of Cylindrical Magnetron.

Fig. 10.1 FM Magnetron Model No. 6A.

Fig. 10.2 Co-axial Magnetron Model No. 7.

Fig. 10.3 Modulation Data on Model 6 No. 31.

Fig. 10.4 Performance Data Model 6 No. 31 Without Modulator Cathode.

THEORETICAL STUDY, DESIGN AND CONSTRUCTION OF C-W MAGNETRONS FOR FREQUENCY MODULATION

QUARTERLY PROGRESS REPORT NO. 2

JUNE, 1950

1. OBJECTIVES FOR THE PERIOD (H. W. Welch, Jr.)

The purpose of this report is to summarize the progress in the University of Michigan Electron Tube Laboratory during the period from March 1, 1950, to June 1, 1950, on Contract No. W-36-039 sc-35561.

The general objectives of the program under this contract are to increase the knowledge of space charge effects and frequency characteristics in c-w magnetrons and apply this knowledge to the development of magnetrons which can be frequency-modulated. Prior to March 1 the emphasis had been on the 2000-2400 mc range. The general technique adopted for development was the use of the magnetron-type space charge as a reactance varying element used in a reactance tube in the same vacuum envelope as the oscillator magnetron. Three models were under development using this principle.

The study of a new method of modulation was initiated on this contract on March 1. This method is essentially the

utilization of the frequency pushing phenomena, or voltage tuning. It was discovered by Wilbur, of General Electric Laboratories, early in 1949, that under certain conditions very wide frequency pushing at uniform power levels is obtainable. The observed frequency shifts have been between 1.5 to 1 and 15 to 1, depending on loading, efficiency and cathode temperature. The frequencies are all below 1000 megacycles. The loading conditions on the tubes have, so far, been quite restrictive, consisting of a load attached directly to the terminals of the anode structure. The Q's are of the order of 10 or less. With a transmission line between the tube and the load it will be quite possible to obtain Q's of the same order in the line which will immediately lead to problems involving long line effect. The objective of the new program is to obtain sufficient understanding of this type of operation that it may be extended to microwave frequencies of 3000 to 4000 megacycles.

In summary the status of work on this contract at the beginning of March was as follows:

(a) The basic understanding of static magnetron type space charge insofar as effects on frequency were concerned was fairly complete, based on experimental and theoretical observations presented in Technical Report No. 1 (issued Nov. 1948) and Quarterly Report No. 1 (see list of reports, page iii). The work was renewed early this year with the purpose of obtaining more rigorous analysis and additional experimental confirmation.

(b) Three designs for frequency modulation magnetrons had been developed. Results on one of these (Model 6) looked

promising. Eight Model 6 tubes have been started in construction. Five of these operated in the desired mode. Modulation data was obtained on two of them. A second type of tube (Model 5) had been constructed but showed little promise. Work on this tube has been dropped for the present. A third model (Model 8) was complete except for cathodes.

(c) A program for studying the magnetron space charge by static methods rather than with r-f had been initiated.

The primary objectives for the period covered by this report were the following:

(a) To make appreciable progress toward and understanding of low Q operation of magnetrons, i.e. frequency pushing, maximum current boundary and temperature-limited operation as related to load.

(b) To design a low power tube usable in study of low Q operation.

(c) Elimination of the loss of power to the modulator cathode in the Model 6 f-m magnetron.

(d) Completion of a Model 8 f-m magnetron.

This report is intended only to report on progress in construction of tubes and development of theory and design during the period. The previously issued reports listed on page iii should be consulted if further information is desired.

2. LOW Q OPERATION OF MAGNETRONS--General (H. W. Welch, Jr.)

The achievement at 500 to 1000 mc of extremely large frequency deviations with low Q magnetrons by voltage tuning, or

frequency pushing, by Wilbur at General Electric Laboratories, has prompted the investigation of the possibility of this type of operation at microwave frequencies (i.e. wavelengths 10 centimeters and shorter). In order to design for a particular frequency range at microwaves, it is desirable to have a better understanding of the fundamental factors involved in obtaining this type of operation. This is usually the case at microwaves since the resonant circuits must assume a closed form, and lumped constant circuits usable below 1000 megacycles gradually must be replaced by distributed constant circuits about 2000 megacycles. It becomes increasingly difficult to have the resonant circuit outside the vacuum envelope.

The most apparent features of the operation obtained at General Electric are the following:

(a) The Q_L is undoubtedly very low. Although no direct measurements of Q are available, it is probable that Q_L's of the order of 10 or less are being used.

(b) The voltage tuning phenomenon is identical with the usually-observed frequency pushing, but is much more pronounced because of the low Q_L.

(c) The low current dropout usually experienced when a magnetron is loaded heavily is conspicuously absent.

(d) The temperature of the cathode must be limited to achieve satisfactory operation. This requires use of a tungsten cathode giving a definite emission boundary. This limitation of emission seems to be intimately related to the maximum current boundary and a required criterion for obtaining

sufficient current.

(e) Efficiency is reduced as bandwidth is increased. This must be due to decreased electronic efficiency since circuit efficiency is obviously very high.

(f) Loading is accomplished right at the tube anode terminals (i.e. almost directly across the capacitive portion of the resonant circuit). Loads farther from the tube may cause trouble with long line effect.

The program of study which has been started in the Michigan Laboratory includes the following. The progress to date will be summarized in the following sections.

(a) Development of a theory of frequency pushing which will permit quantitative, or at least semi-quantitative predictions to be made about particular designs.

(b) Determination of the causes of current dropout as they are related to loading.

(c) Investigation of the effect of temperature-limited cathode operation on the fundamentals of space charge behavior in an oscillating magnetron.

(d) Experimental study of tubes specially built for low Q_L operation with emphasis on the above three points and a study of long line effects.

(e) Development of design criteria based on these findings if low Q operation at microwave frequencies seems feasible.

3. FREQUENCY PUSHING (H. W. Welch, Jr.)

The ideas in the present section should not be

accepted as final but should represent progress to date in the development of a theory of frequency pushing.

The phenomenon of frequency pushing can be discussed in terms of two sets of fundamental concepts, one involving an approximate picture of the magnetron space charge, and the other involving the equivalent circuit of the magnetron. Figure 3.1 gives a conceptual picture of the space charge under three different load conditions. Figure 3.2 is an equivalent circuit which is useful in relating the space charge swarm properties to the circuit. In Figure 3.3 a set of data is reproduced from Technical Report No. 1 which illustrates nicely the effects to be described. These data are the result of hot impedance measurements carried continuously into pushing measurements on a QK-59 magnetron. In the hot impedance measurements resonant wavelength is measured by feeding in an external signal and by making the usual standing wave ratio and position of minimum measurements to determine resonance. When oscillation starts, pushing is measured as the oscillatory wavelength as a function of plate voltage instead of plate current (which is, however, also measured) in order that comparison with the hot impedance test may be made on the same scale.

These data may be interpreted in the following manner. As anode voltage is increased from zero, the resonant wavelength increases slowly because of the increase in capacitance caused by the increase in diameter of the dense hub of the space charge swarm. The electrons in this hub are proceeding around the cathode at sub-synchronous angular velocities, i.e. the

angular velocity of the boundary space charge swarm is less than the angular velocity of the traveling electromagnetic wave due to the impressed radio frequency which goes around the interaction space in the same direction. At about 450 volts these two velocities became synchronous and above 450 volts the electrons would normally be going faster than synchronism. However, if the impressed radio frequency signal is strong enough, which is apparently the case, the normally faster-than-synchronous electrons will be slowed to synchronism, forming a synchronous swarm of space charge as described in Technical Report No. 1, section 5, case II. The synchronous space charge swarm should form in spokes, because electrons will be slowed down only in regions of retarding field and thus drift outward and back to a position of equilibrium in the positive potential region of the traveling wave. In regions of accelerating field the electrons will be speeded up and sent back toward the cathode by the Lorentz force. As anode voltage is raised the spoke will grow outward, still maintaining the same phase relationship with the wave provided no power is continuously transferred by the space charge swarm to the radio frequency field. At approximately the Hartree voltage the space charge spoke will just reach out to the anode. The effect of the presence of the spoke is to cause an induced current to appear in the anodes. The maximum value of current leads the maximum positive potential by 90 degrees if the spoke is in the position shown in Figure 3.1a. This follows from the observation that when a spoke passes under an anode at maximum positive potential, the current changes

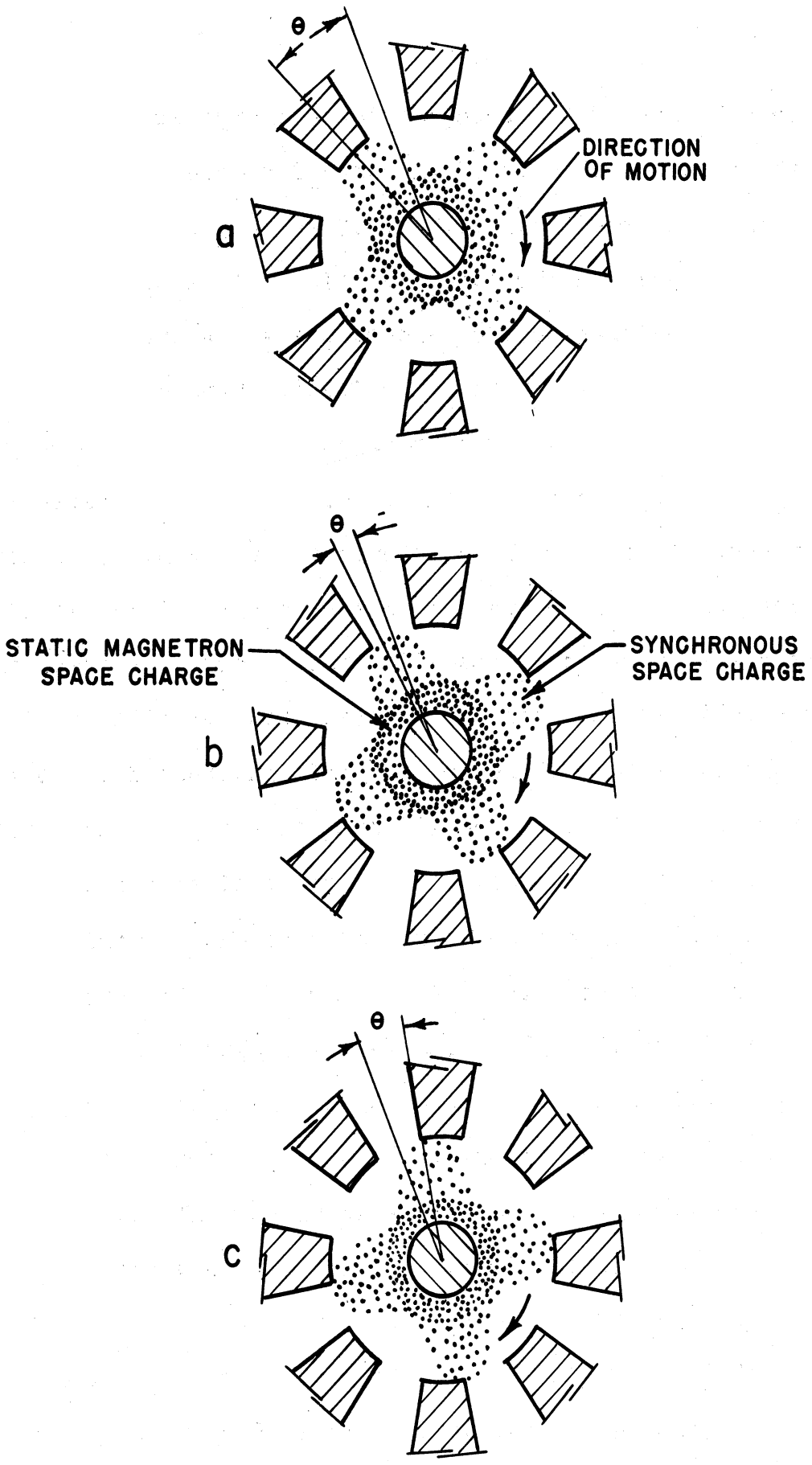

FIG. 3.1
PICTORIAL REPRESENTATION OF SPACE CHARGE WITHIN INTERACTION SPACE.

from positive to negative. Thus the expanding spoke should increase the effective capacitance of the system since it contributes a leading current. The extension of the spoke occurs more rapidly with voltage than the expansion of the cloud which accounts for the relatively rapid increase of the resonant wavelength after the synchronous voltage is reached. Also the fact that the effect is capacitive is not dependent on the density of the space charge but on the position at which the spoke is formed. The effect of the hub, as has been pointed out in previous reports, may be either to increase or decrease the resonant wavelength, depending on density of the space charge. Curves illustrating this point were given in Quarterly Report No. 1.

As soon as the spoke reaches out to the anode there can be a transport of electrons through the spokes and consequently a net delivery of power from the spokes to the radio frequency field. It will thus be necessary for the current induced by the rotating spoke to have a component in phase with the r-f voltage. Since output power is in general increased by raising the anode voltage, the electrons in the spoke will tend to speed up relative to the motion of the swarm so the spoke will tend to advance in phase. This is indicated in Figure 3.1b. The angle θ between the spoke and the position of maximum r-f field is now smaller; an appreciable current exists in phase with the r-f voltage and power is delivered. The capacitive effect of the spokes is decreased and the resonant wavelength is changing back toward

the cold resonant frequency of the tank circuit. As the angle θ goes to zero the space charge swarm will deliver maximum power since the electrons are moving in the maximum decelerating field. The resonant frequency will then be the resonant frequency of the tank circuit since the current is in phase with the r-f voltage. If the anode voltage is increased beyond this point, the spoke will still tend to speed up and the angle θ will become negative. Power delivery will fall off and the resonant wavelength will be below the cold resonant wavelength of the tank circuit. This position of the spoke is indicated in Figure 3.1c. According to Wilbur, this type of behavior has been noticed on the G.E. magnetrons. That is, the frequency is pushed through the cold resonant frequency of the tank circuit and power output goes through a maximum.[1]

The above speculation involving behavior of the space charge swarm intimates that the observed effects are caused by the shifting in phase of the space charge spokes relative to the r-f voltage maximum. In other words, the configuration and density of the spoke remains constant and is independent of magnitude of r-f voltage. This is conceivable but probably not so. However, if it is not quite so, the qualitative description of the behavior just given will still hold, with modification.

---

1 Note that the condition for $\theta = 0$ may not be quite the cold resonant frequency of the magnetron due to effects of the hub of space charge and temperature effects.

Actually the assumption that the configuration and density of the synchronous space charge swarm is relatively independent of r-f voltage is equivalent to stating that the magnetron space charge swarm is a constant current generator. This has long been assumed to be approximately true. Figure 3.2 shows a simple equivalent circuit which is useful in the discussion of this property.

The input admittance of this circuit seen from the terminals T - T' is given by the following:

$$Y_T = \frac{I_g}{E_T}\angle\phi = \frac{Y_{oc}}{Q_L}\sqrt{1 + 4\delta\ Q_L^2}\ \underline{\angle \tan^{-1} 2\delta\ Q_L} \qquad 3.1$$

This notation implies that the magnitude of the current delivered is not necessarily a function of the phase angle between the current and voltage, ϕ. The other symbols used in the expression are defined as follows:

$$Y_{oc} = \omega_o C \quad \text{where } \omega_o = 1/\sqrt{LC}$$

$$\delta = \frac{\omega - \omega_o}{\omega_o} = \frac{\lambda_o - \lambda}{\lambda_o}$$

$$Q_L = \frac{Y_{oc}}{G_T + G_L}$$

The various factors in this equation are plotted in Figure 3.4

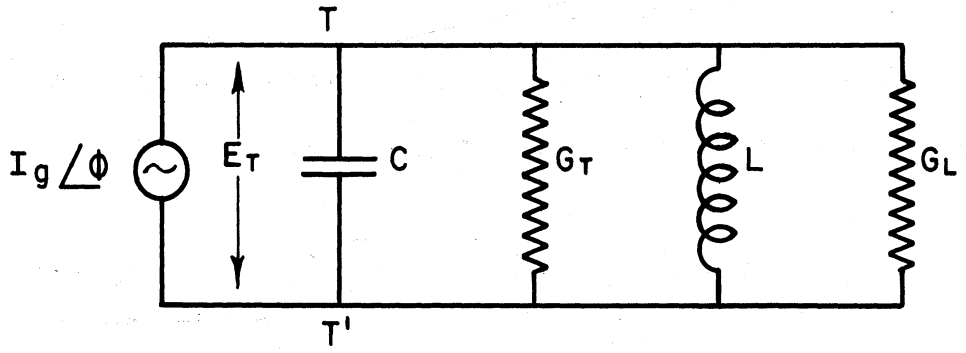

FIG. 3.2
EQUIVALENT CIRCUIT FOR OSCILLATING MAGNETRON

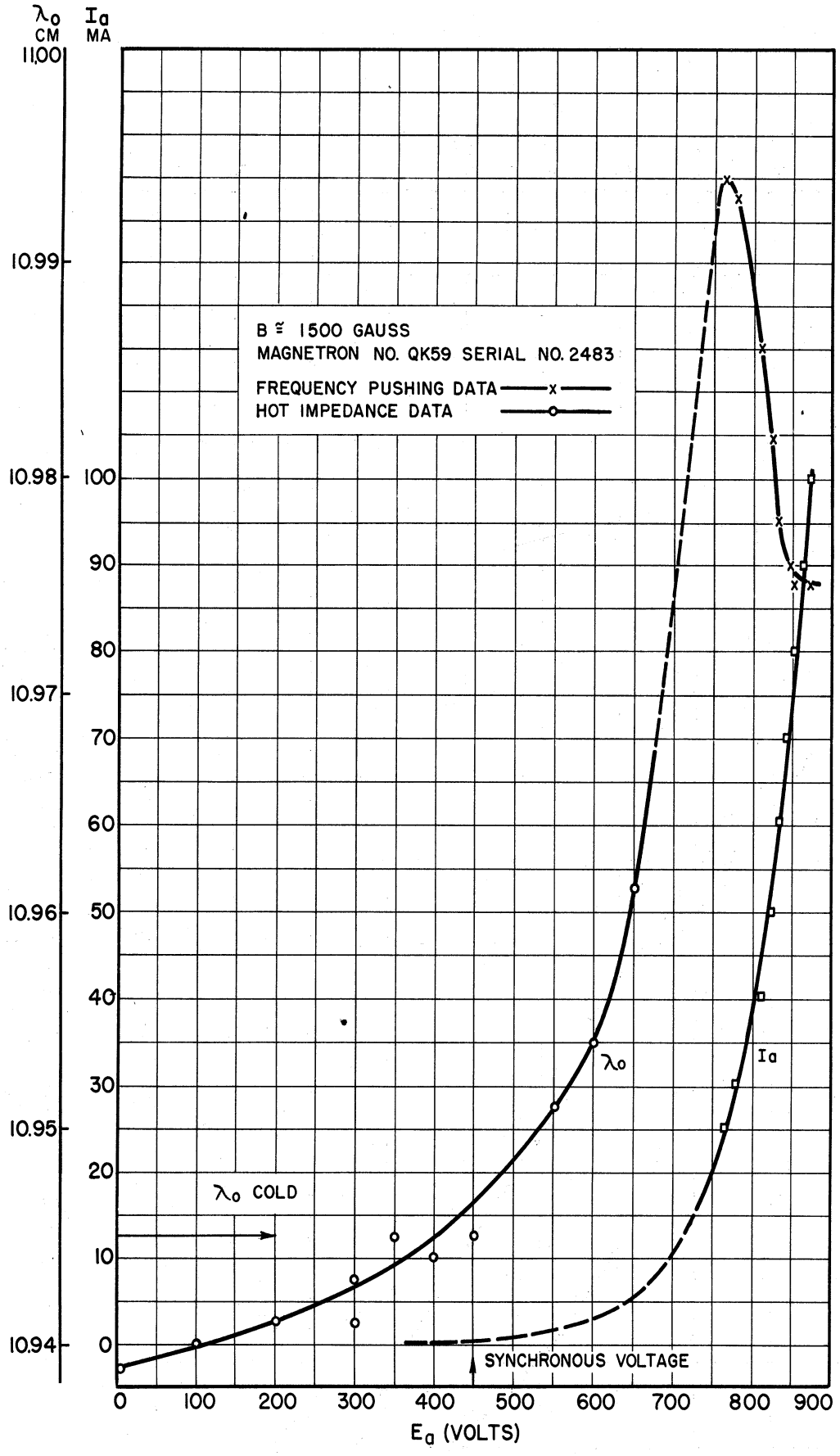

FIG. 3.3

CHANGE OF MAGNETRON RESONANT WAVELENGTH WITH PLATE VOLTAGE

COMPARISON OF FREQUENCY PUSHING AND HOT IMPEDANCE TEST RESULTS

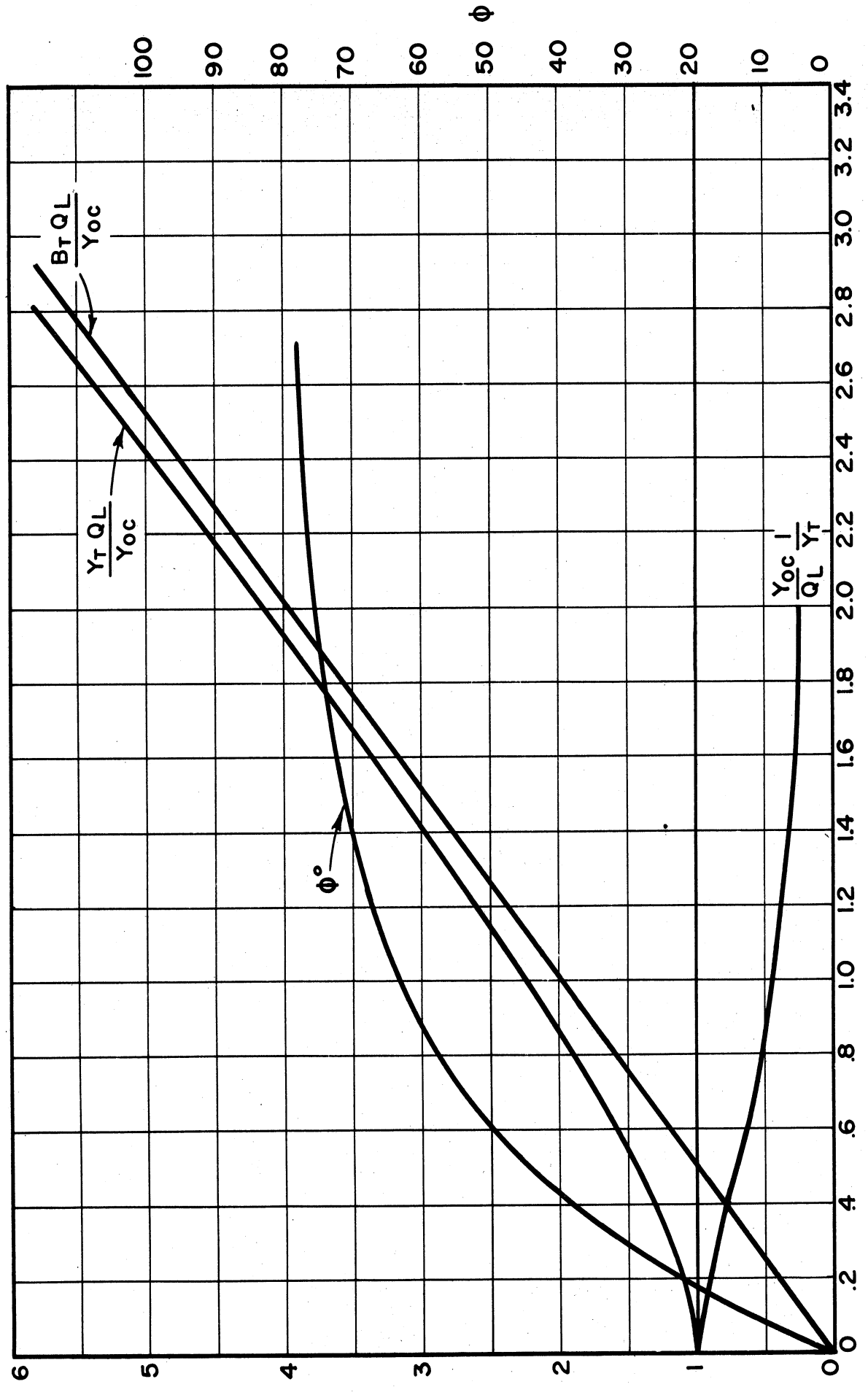

FIG. 3.4 PARAMETERS INVOLVED IN EQUATION 3.1 APPLYING TO CIRCUIT OF FIG. 3.2

The r-f voltage at T - T', i.e., between anode sets in the magnetron is given by

$$E_T = \frac{I_g}{\frac{Y_{oc}}{Q_L}\sqrt{1 + 4\delta^2 Q_L^2}}$$

The power delivered to the load is given by

$$P_L = E_T^2 \; G_L$$

or

$$P_L = \frac{I_g^2}{(Y_{oc}/Q_L)^2 \; (1 + 4\delta^2 Q_L^2)} \qquad 3.2$$

G_L may be written in terms of external Q for matched load.

$$G_L = \frac{Y_{oc}}{Q_e} \qquad 3.3$$

Q_e can be determined from the measurable Q's, unloaded and loaded, by the following:

$$\frac{1}{Q_e} = \frac{1}{Q_L} - \frac{1}{Q_o} \qquad 3.4$$

TABLE 3.1

Data for Figure 3.5

Magnetron Model 3, Serial No. 8, June 7, 1950

	$\lambda - \lambda_o$ ($\lambda_o = 16.77$)			P_L	I_{max}	E_b	$\Delta\lambda$
	200 ma	100 ma	0 ma	200 ma	ma	20 ma	0-200 ma
1	-.063	-.085	-.180	225	375	1670	-.117
2	-.065	-.090	-.170	215	475	1580	-.105
3	-.104	-.145	-.250	170	200	1600	-.146
4	-.205	-.243	-.315	115	200	1520	-.110
5	-.130	-.160	-.250	92.5	450	1500	-.120
6	-.116	-.135	-.190	80	600	1520	-.074
7	-.050	-.060	-.135	100	725	1580	-.085
8	-.000	-.243	-.085	158	600	1600	-.085
9	+.050	-.248 +.010	-.390	175	400	1540	-.440
10	-.180	-.230	-.310	105	200	1550	-.130
11	-.157	-.172	-.255	100	375	1500	-.098
12	-.065	-.083	-.155	87.5	675	1500	-.090
13	-.015	-.028	-.120	173	525	1600	-.105
14	-.065	-.086	-.156	105	700	1540	-.091
15	—	—	-.008	—	.075	1800	—
16	-.146	-.150	-.220	225	200	1640	-.074
17	-.126	-.135	-.185	163	475	1590	-.059
18	-.022	-.025	-.060	255	450	1690	-.038
19	-.066	-.090	-.125	135	775	1600	-.059

1ST NUMBER BY POINT GIVES PUSHING IN CM. BETWEEN I_b=0 AND I_b= 200 MA.

2ND NUMBER GIVES MAX. CURRENT BOUNDARY IN AMP.

$\Delta\lambda$ GIVEN FROM λ_o = 1677 CM AT I_b = 100 MA

P_L MEASURED AT I_b= 200 MA.

E_{bt} = STARTING VOLTAGE.

TUBE AT $-2\lambda_o$

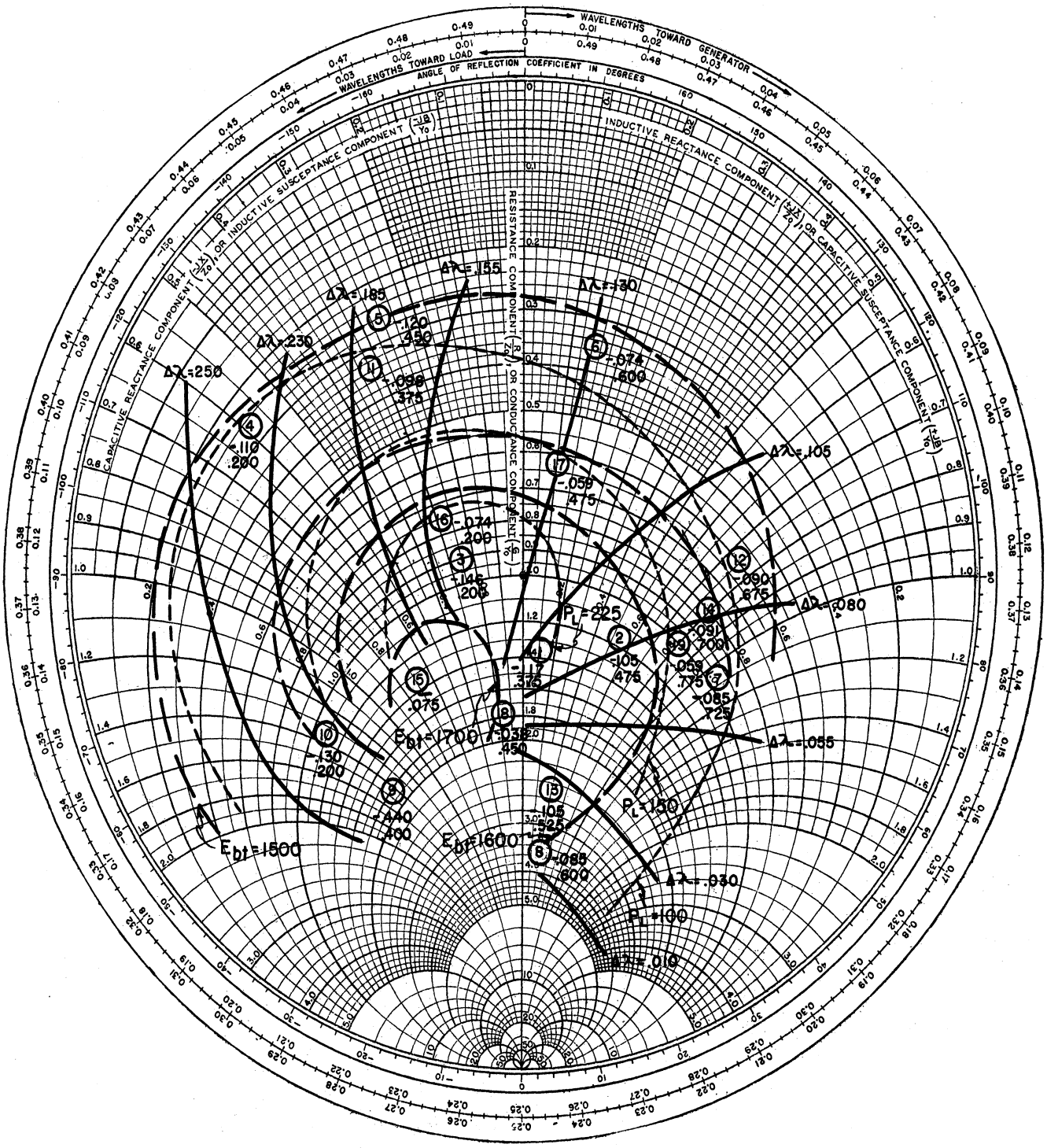

FIG. 3.5 LOAD DIAGRAM MODEL 3 #8

TABLE 3.2

Complete Pushing Data for Curve of Figure 3.6

E_b volts	I_b amp.	λ cm.	$\frac{\lambda - \lambda_o}{\lambda_o} \times 100$ (λ_o=16.77) per cent	$\eta E_b I_b$ (η= 58%) watts	$.23 \frac{1500}{1+4.10^2\delta^2}$ watts
1600	.020	16.95	1.07	18.5	60.3
1670	.050	16.880	.658	48.5	125
1750	.100	16.855	.506	101	171
1900	.200	16.833	.376	220	220
2050	.300	16.827	.340	357	237
2200	.375	16.805	.208	480	290

A series of measurements of pushing have been made for various values of loads in order to determine the effect of the various parameters. These results are summarized on the Rieke diagram of Figure 3.5. Analysis of the overall behavior is not complete; however, the possible applicability of the simple theory just given is demonstrated by a discussion of one point near a matched load. Point No. 1 is chosen.

The pushing curve for point No. 1 is given in Figure 3.6, Curve No. 1. Power is used instead of current as a variable in order to more readily check the theory. Power was measured at only one current, however, and efficiency is assumed constant. Thus, $P_L = \eta E_b I_b$, where η = overall efficiency.

For the tube on which these measurements were made,

Y_{oc} = .00555 mhos

Q_L = 100

Q_o = 600

Q_e = 120

λ_o = 16.770 resonant wavelength cathode hot, space charge swarm hub not accounted for

η = 58% = overall efficiency at I_b = 200 ma (P_L = 230 watts)

$\frac{Q_L}{Y_{oc}}$ = 1800 ohms

$\frac{1}{G_L} = \frac{Q_e}{Y_{oc}}$ = 2160 ohms

Using these values Equation 3.2 becomes

$$P_L = 1500\, I_g^2 \frac{1}{1 + 4.10^4 \delta^2}$$

or

$$\eta E_b I_b = I_g^2 \frac{1500}{1 + 4.10^4 \delta^2} \qquad 3.5$$

Equation 3.5 is plotted for comparison with the data in Figure 3.6, Curve No. 2 for $I_g^2 = 2.3$ and efficiency assumed constant at 58 per cent. This value is selected to make the curves coincide at 220 watts. It is obvious that the assumption that I_g is a constant current is not valid.

It is possible to carry the data a step further to arrive at more definite conclusions about the behavior of the current generator. Let us assume that

$$(I_g)^2 = K(P_L)^b \qquad 3.6$$

Then Equation 3.2 may be written

$$P_L = K(P_L)^b \frac{Q_L^2}{Y_{oc}^2} G_L \frac{1}{1 + 4\delta^2 Q_L^2} \qquad 3.7$$

or

$$\log \left(\frac{Q_L^2}{Y_{oc}^2} \frac{G_L}{1 + 4\delta^2 Q_L^2} \right) = (1 - b) \log P_L - \log K \qquad 3.8$$

If the data used in plotting Curve No. 1 in Figure 3.6 is plotted on log log paper the slope should be (1 - b) and the intercept (-log K). This is done in Figure 3.7. The resulting relationship for the current is

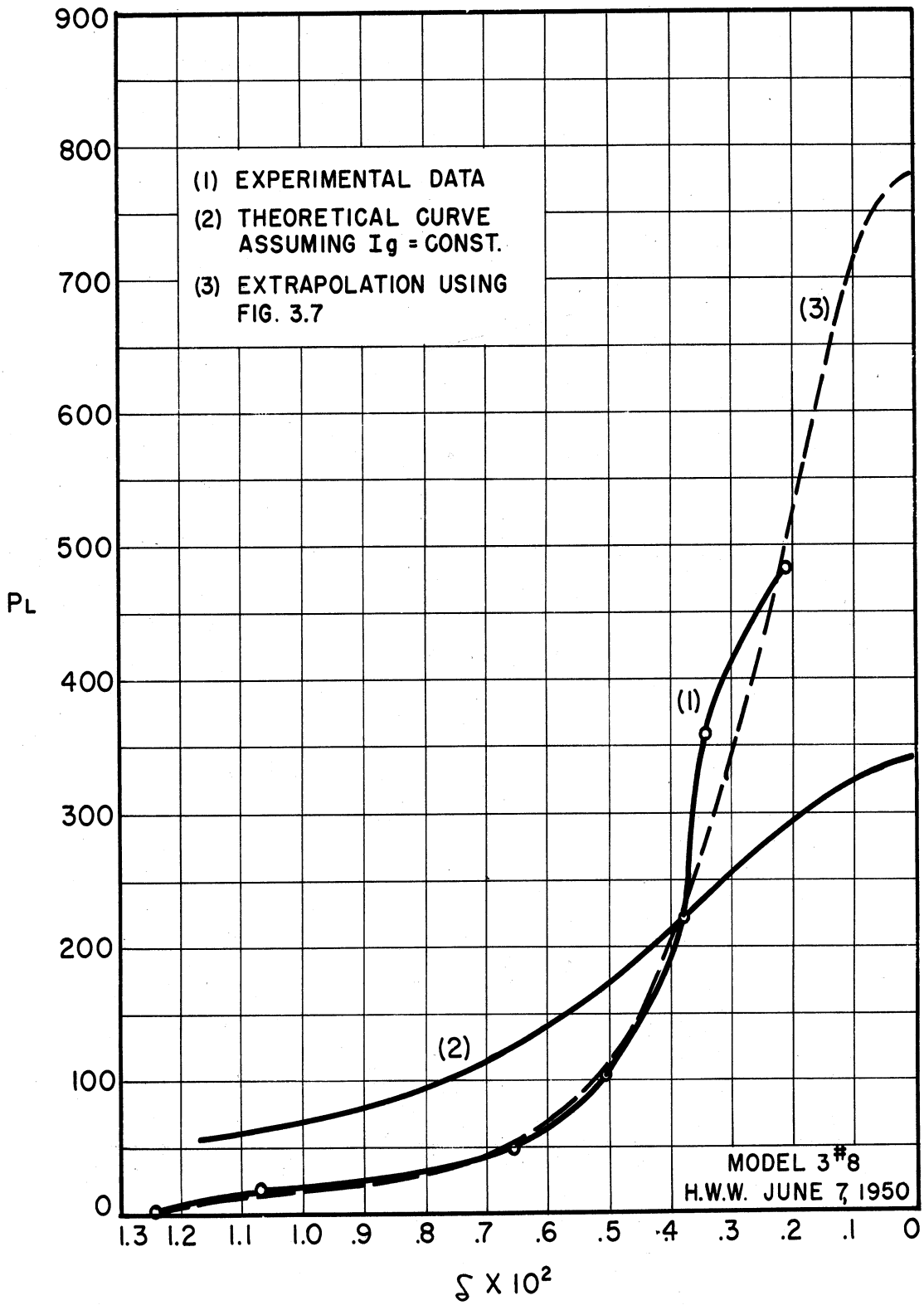

FIG. 3.6 COMPARISON OF PUSHING DATA AND THEORY

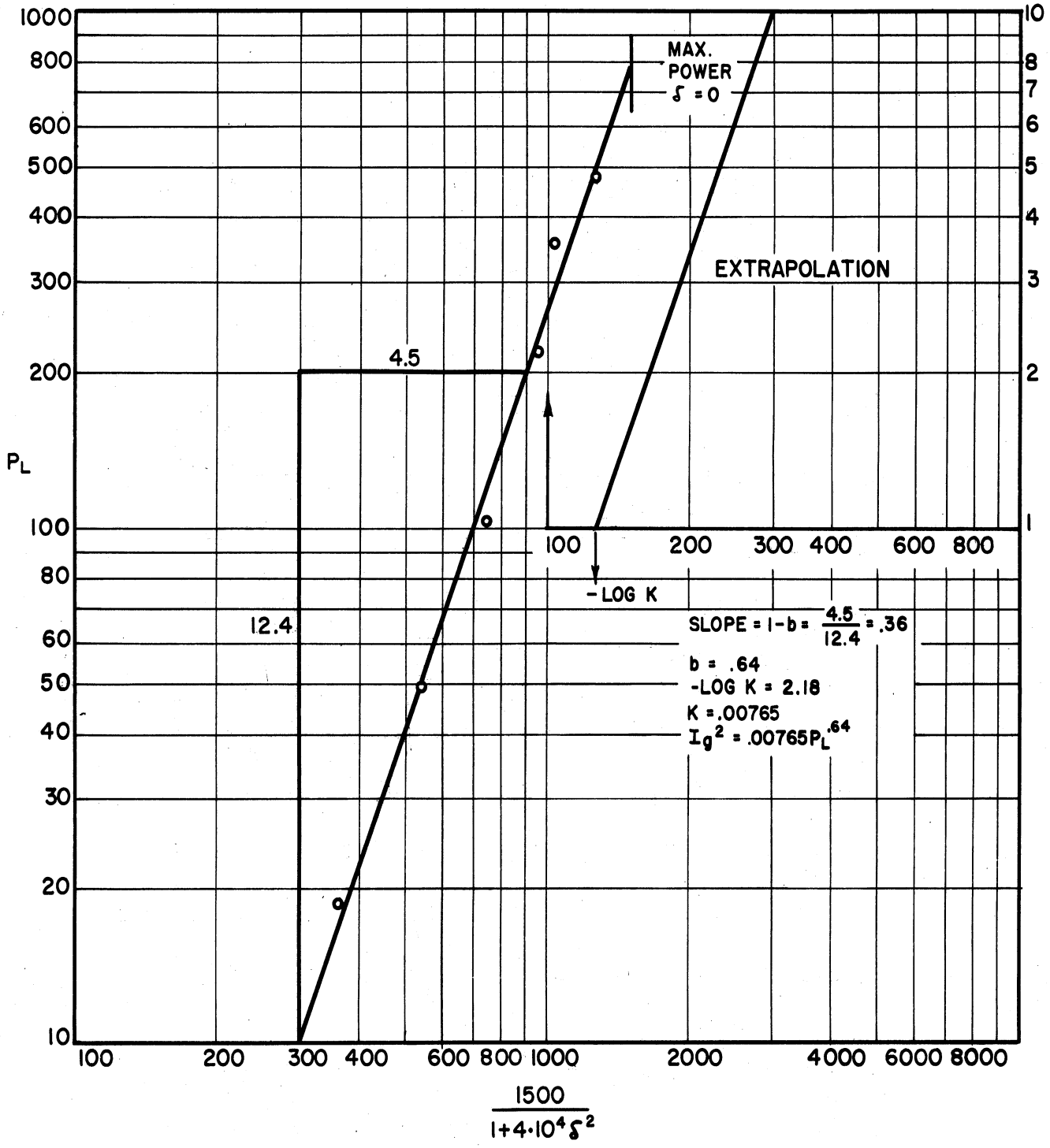

FIG. 3.7 LOGARITHMIC PLOT OF DATA FROM TABLE 3.2

$$I_g^2 = .00765\ P_L^{.64}$$

or

$$I_g = .0874\ P_L^{.32} \qquad 3.9$$

The current in this particular case is approximately proportional to the 2/3 power of the r-f voltage between segments. It remains to be seen if this relationship can be applied to other magnetrons. The straight line of Figure 3.7 is replotted on the coordinates of Figure 3.6 as Curve No. 3, and indicates the expected extrapolation of Curve No. 1.

An important point which should be noted is that the horizontal scale in Figure 3.6 is essentially $\delta\ Q_L$ since $Q_L = 100$. Everything else remaining the same, therefore, if Q_L were reduced to 10 the frequency deviation would be multiplied by 10. This change would have to be made with a corresponding change in Y_{oc} to keep the ratio of I_g to E_T constant.

More data will be taken in the near future to check these possibilities. It is to be expected that a more complex analysis involving the geometry of the interaction space will be needed since field configurations for the same r-f voltage and loading could be very different for different tube geometries.

The current given by Equation 3.9 is plotted in Figure 3.8 along with the phase angle of the current generator. A rather interesting result of this experiment is that

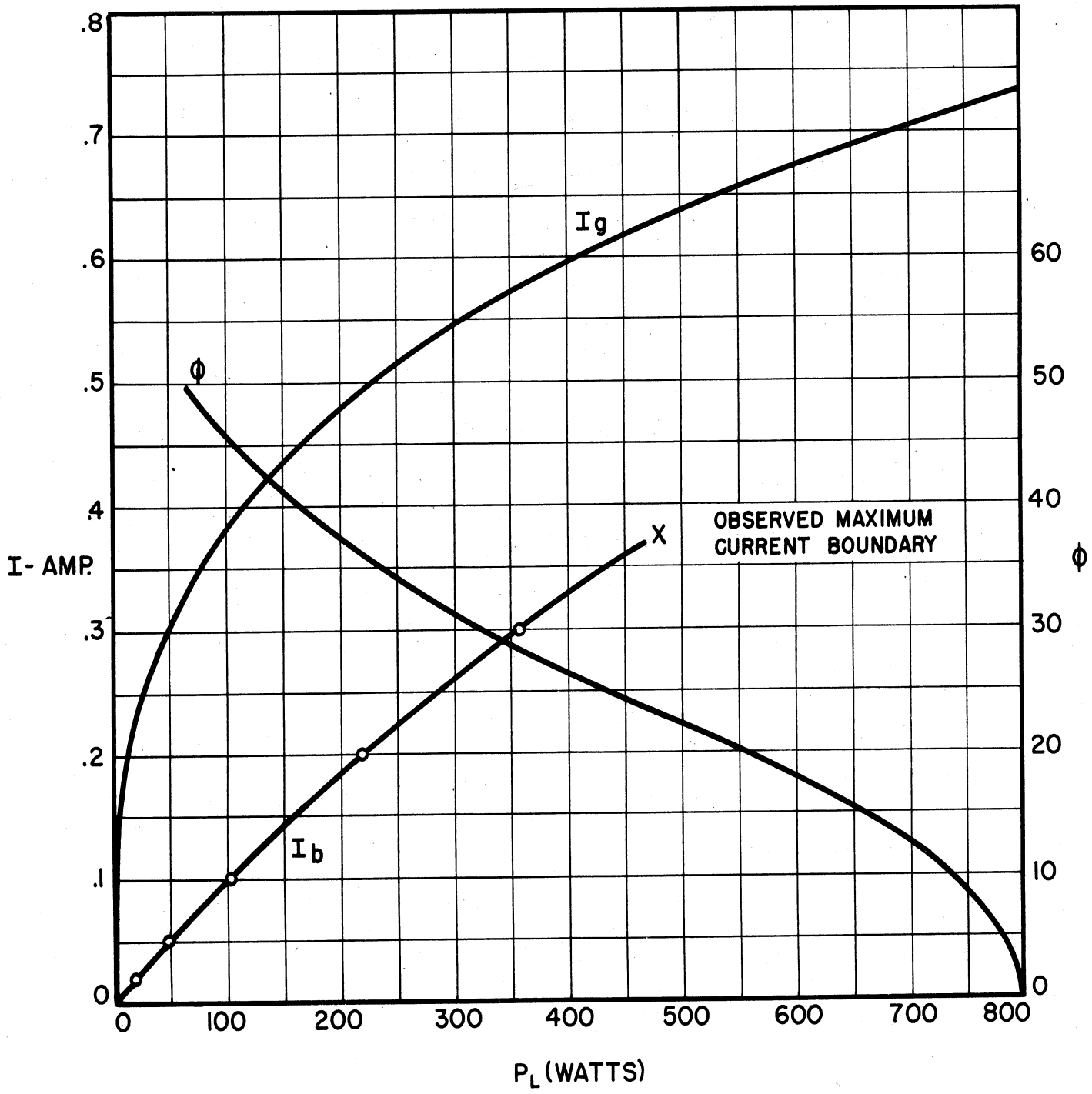

FIG. 3.8 GENERATOR CURRENT (Ig) CALCULATED FROM EQUATION 3.9 COMPARED WITH I_b AND PHASE ANGLE ϕ AS A FUNCTION OF LOAD POWER.

the current generator output is a factor of two or more greater than the average d-c current, which is plotted for comparison. This is possible in a generator which induces current into the load. In fact it would be possible to have zero average current and finite induced current 90 degrees out of phase with the voltage.

4. MAXIMUM CURRENT BOUNDARY--General (H. W. Welch, Jr.)

There are several factors which are known to be involved in the determination of maximum current boundary for magnetrons. Most of these which have been studied in any detail apply particularly to pulsed tubes and have no meaning in c-w operation. In the present problem where operation at very low Q's is involved, the maximum current boundary is apt to be the limiting factor. Therefore it seems advisable to study in some detail the underlying causes of the maximum current boundary in c-w magnetrons in order to find the proper way to design without this limitation.

The initial study has been carried on with the intent that a general understanding of the factors involved will be obtained after which each factor will be studied until it is understood well enough to be subject to control. Discussions with engineers from other laboratories, particularly Mr. Edward Dench and Mr. W. C. Brown of Raytheon, have been extremely helpful. Extensive experimental data on maximum current boundary were provided by Mr. Dench. As a result of this initial study the following five factors are suggested as being particularly important in determination of

maximum current boundary in c-w magnetrons.

a. Cathode limitation of available current. This is usually a thermionic emission limitation but may be made more complex by enchanced emission such as that observed by Mr. Jepson of Columbia Radiation Laboratory.[1]

b. Space charge limitation of available current. This is the current which, assuming no saturation at the cathode, may be passed through the space charge swarm in the magnetron as determined by the voltage at the edge of the swarm.

c. Induced current limitation placed by the maximum possible density and extent of space charge in the spokes. This is actually not a maximum current boundary but a maximum power boundary. However, it is possible that as the maximum power boundary is reached something would happen to the focussing action of the fields in the spokes to cause current dropout.

d. Transit time limitation of current through the spokes. In order to supply the conduction current necessary to supply power to the system a certain number of electrons must be collected during each cycle of operation. This requires that the average radial velocity have a certain minimum value dependent on the average space charge density in the spokes. If the minimum radial velocity reaches the value determined roughly by the radial length of the spoke divided by the minimum time of transit through the spoke the

---

1 Columbia Radiation Laboratory Quarterly Report, March, 1950, page 2.

conduction current will be a maximum. Further increase in voltage will then be expected to cause current dropout.

e. Mode competition, causing current dropout in one mode when another mode is more favorable to the magnetron oscillation.

f. Debunching due to insufficient focussing action by the r-f field as the spoke changes in position and the current increases.

The method of control of two of these factors is immediately obvious. Cathode limitation of current can be rectified by provision of adequate emission, and mode competition can be eliminated by provision of adequate mode separation. The question which arises is how much is adequate. According to Mr. Brown of Raytheon, experience indicates that a voltage mode separation of greater than 17 per cent is sufficient. This separation depends on loading, however, and should be investigated further. The problem of the cathode is also not completely obvious since it is experimentally observed that when the measured diode emission is from three to six times the average current drawn by the magnetron the temperature begins to have an effect on the maximum current boundary. This may have some very subtle interpretation but it is probable that it is related to the peak currents drawn during the r-f cycle similar to the comparable limitation in ordinary class C operation.

Very little is understood about the induced current limitation, the transit time limitation and the debunching

phenomenon, and, so far as we know, no experimental data definitely related to these effects exist. The data discussed in the last section can be related to maximum current boundary. It is interesting to note that the current dropout occurs for $\delta \times 10^2 = -0.2$. This means that the maximum power boundary due to the induced current limitation was not reached. However, if presence of the space charge hub were accounted for, it is quite likely that the resonant wavelength in operation would be shifted to $\delta \times 10^2 = -0.2$ since this is about the order of magnitude and the direction such a shift would take. If this is not the case one of the other causes of current dropout must apply. From a theoretical point of view it is necessary to know more about the exact configuration of the spokes and the transit time of the electron. The space charge density and the radial extent of the spokes should be approximately calculable from the theory given in Technical Report No. 1. (Equations 5.20 and 5.30). These problems will be studied further.

The space charge limitation of current has been given more detailed study and is treated in the next section.

5. SPACE CHARGE LIMITED CURRENT LIMITATION IN THE OSCILLATING MAGNETRON (H. W. Welch, W. Peterson)

Measurements at the M.I.T. Radiation Laboratory led Slater and others to suggest the empirical space charge limitation current of 1/2 the Allis current in the oscillating magnetron. The Allis current is the space charge limited current

at the cutoff voltage in the static magnetron. The following analysis results in a method for theoretical calculation of the space charge limited current in an oscillating magnetron.

The physical assumptions are based on the picture of the space charge swarm presented in Figure 3.1. It is assumed that the radius of the hub of the space charge swarm is that radius at which the electrons first reach angular velocities synchronous with the electromagnetic wave traveling around the interaction space. This radius is determined by the magnetic field by the following relationship

$$\frac{B}{B_o} = \frac{1 - \frac{r_c^2}{r_a^2}}{1 - \frac{r_c^2}{r_n^2}} \qquad 5.1\,*$$

The potential at the edge of the swarm is given by the following

$$\frac{E_n}{E_o} = \frac{r_n^2}{r_a^2} \qquad 5.2\,*$$

In these equations

r_n = radius of swarm where electrons reach synchronism with r-f field

r_a = anode radius

---

* The starred formulae are discussed in Technical Report No. 1

r_c = cathode radius

E_n = potential at edge of synchronous swarm corresponding to the energy of the electron attributable to angular velocity

$$E_o = \frac{1}{2} \frac{m}{e} \frac{2\pi c}{n\lambda} r_a^2 \qquad 5.3$$

n = mode number = total phase shift around interaction space divided by 2π

$$B_o = 2 \frac{m}{c} \frac{2\pi c}{n\lambda} \frac{1}{1 - \frac{r_c^2}{r_a^2}} \qquad 5.4$$

B = applied magnetic field

It is convenient to use as a reference the space-charge-limited current as derived by Langmuir for a non-magnetic diode. This current is defined as follows for E_o on the anode.

$$I_{LO} = 2\pi \times 2.331 \times \frac{L}{r_a} \times \frac{E_o}{\beta_a^2} \qquad 5.5$$

where

L = the length of the emitting surface

E_a = the anode voltage

β_a = a function of the ratio r_a/r_c defined by Langmuir and given in almost any text on vacuum tube electronics.

If we define further

E_H = voltage corresponding to the energy of an electron with synchronous angular velocity

at the anode, or 'cutoff' voltage

I_{La} = Langmuir current with E_H applied

we have the following relationships for the static magnetron

$$\frac{I_{La}}{I_{LO}} = \left(\frac{E_H}{E_o}\right)^{3/2} \qquad 5.6$$

and

$$\frac{E_H}{E_o} = \left(\frac{B}{B_o}\right)^2 \qquad 5.7^*$$

With the assumption that the potential corresponding to the energy of radial motion of the electrons is very small compared to E_n, we may write the following

$$\frac{I_{Ln}}{I_{LO}} = \left(\frac{E_n}{E_o}\right)^{3/2} \frac{r_a}{r_n} \frac{\beta_a^2}{\beta_n^2} \qquad 5.8$$

$$\beta_a^2 = \beta^2 \left(\frac{r_a}{r_c}\right)$$

$$\beta_n^2 = \beta^2 \left(\frac{r_n}{r_c}\right)$$

I_{Ln} is the Langmuir current in a diode with anode at r_n and voltage E_n applied. In order to relate these currents to the magnetron the Langmuir current must be related to the space charge limited current for a magnetic diode. This has

---

* The starred formulae are discussed in Technical Report No. 1

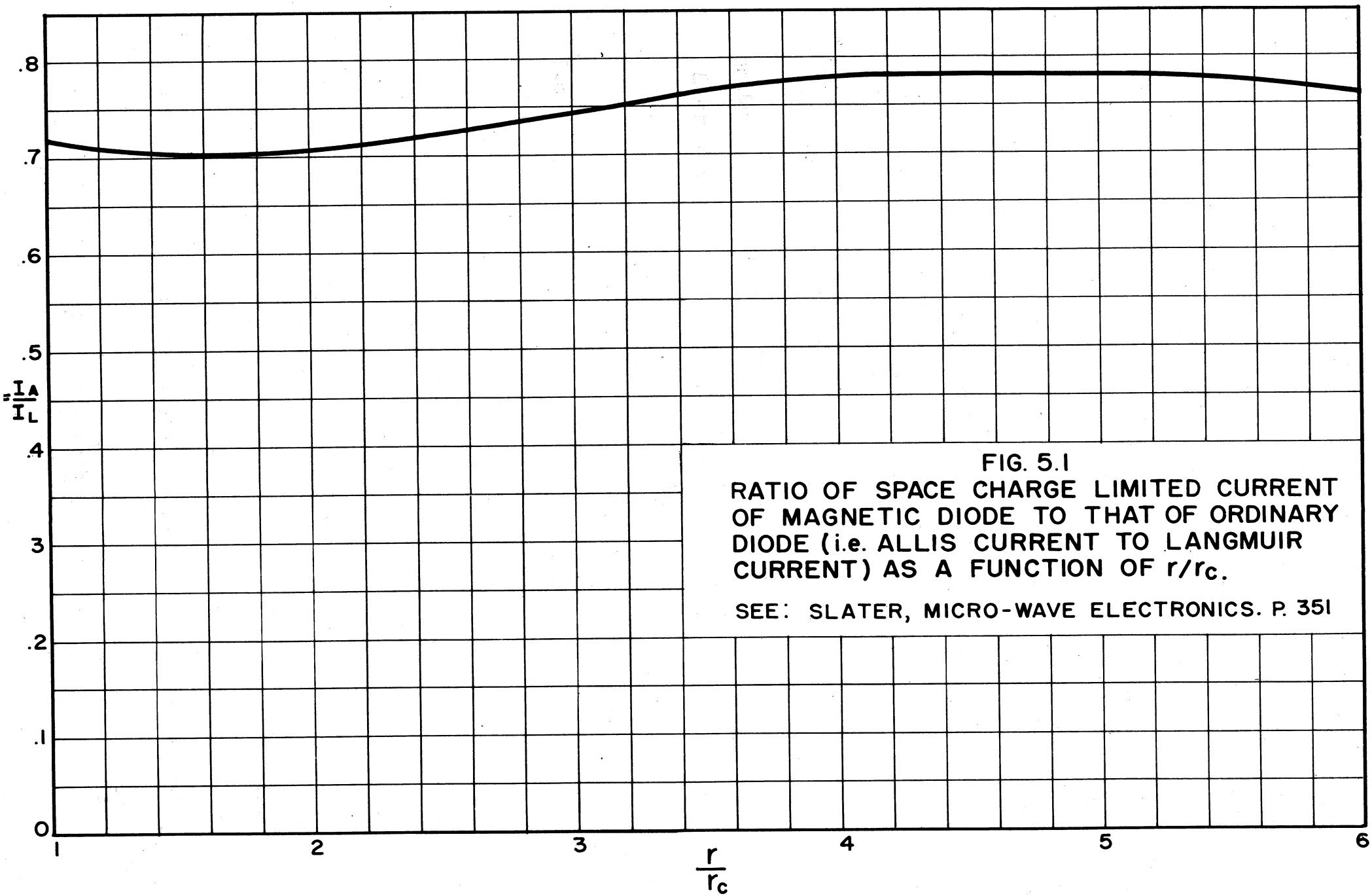

FIG. 5.1
RATIO OF SPACE CHARGE LIMITED CURRENT OF MAGNETIC DIODE TO THAT OF ORDINARY DIODE (i.e. ALLIS CURRENT TO LANGMUIR CURRENT) AS A FUNCTION OF r/r_c.

SEE: SLATER, MICRO-WAVE ELECTRONICS. P. 351

been shown by Allis,[1] Page and Adams[2] and Brillouin[3] with general agreement to have a value given by

$$I_A = \alpha I_L \qquad 5.9$$

where α is a function of r/r_c, shown in Figure 5.1. Note that α has the value of 0.72 for a plane magnetron and 0.86 for a cylindrical magnetron with infinitely small cathode. For conventionally used values of r_a/r_c in the magnetron $\alpha = 0.71$. The space charge limited current for the magnetic diode defined by 5.9 is usually called the Allis current.

It becomes apparent that the current we wish to define is given by

$$I_{An} = \alpha_n I_{Ln} \qquad 5.10$$

where I_{An} is the maximum space charge limited current which can be drawn through the hub of the rotating space charge wheel in the oscillating magnetron, and I_{Ln} is given by Equation 5.9. $\frac{I_{Ln}}{I_{Lo}}$ may be conveniently plotted using the

---

1 Microwave Electronics, J. C. Slater, section 13.7, page 345.

2 "Space Charge in Plane Magnetron", Page and Adams, Physical Review, V69, page 492, 1946.

"Space Charge in Cylindrical Magnetron", Page and Adams, Physical Review, V69, page 494, 1946.

3 "Electronic Theory of the Cylindrical Magnetron," OSRD 4742, AMP Report 129-2R.

"Electronic Theory of Plane Magnetron", AMP Report 129-1R.

"Oscillations in a Plane One-Anode Magnetron", OSRD 5173, AMP Report 129-3R.

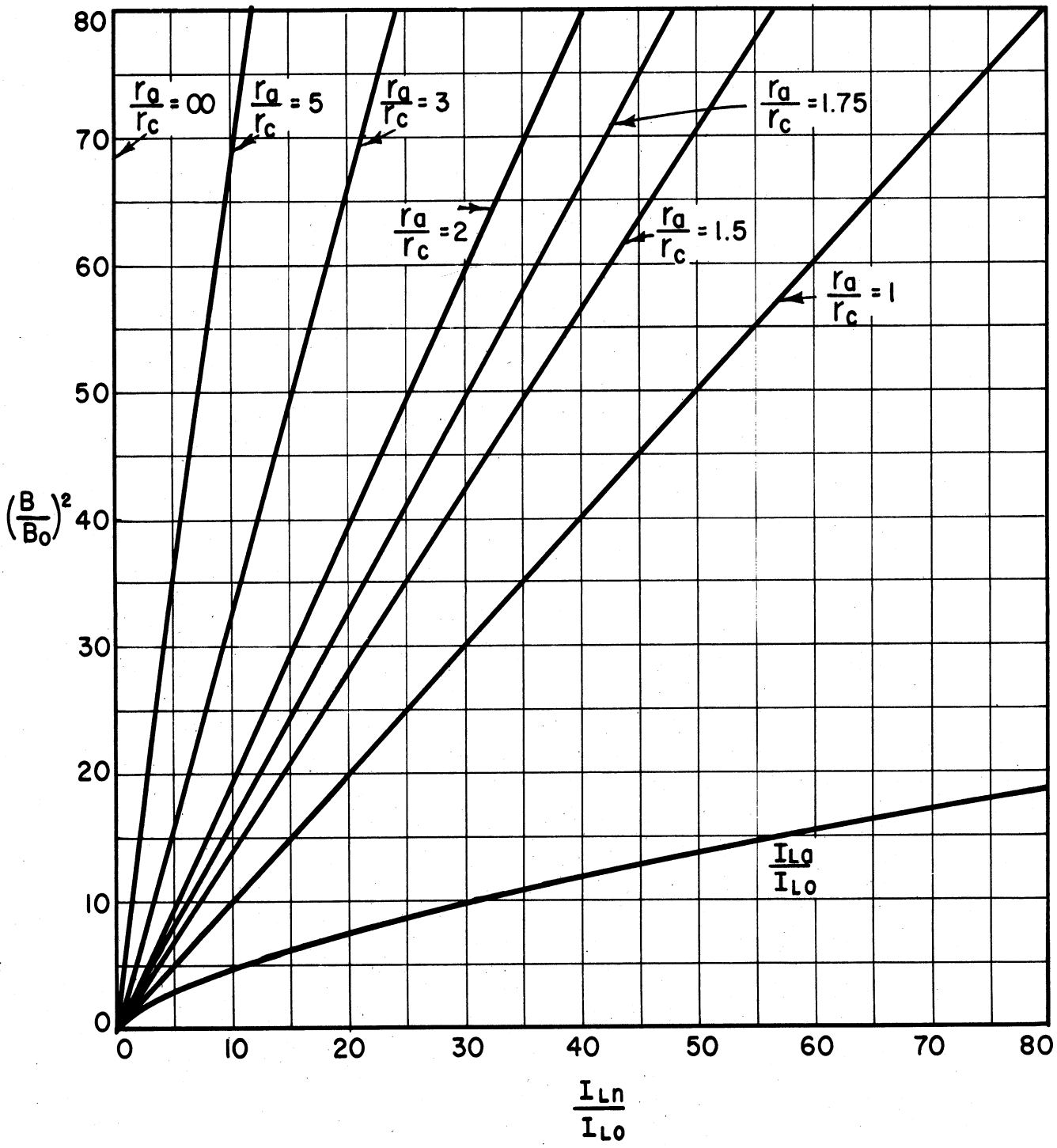

FIG. 5.2 SPACE CHARGE LIMITED CURRENT IN OSCILLATING MAGNETRON FROM EQUATIONS 5.1 AND 5.2

$\left(\frac{B}{B_0}\right)^2$ USED AS A VARIABLE

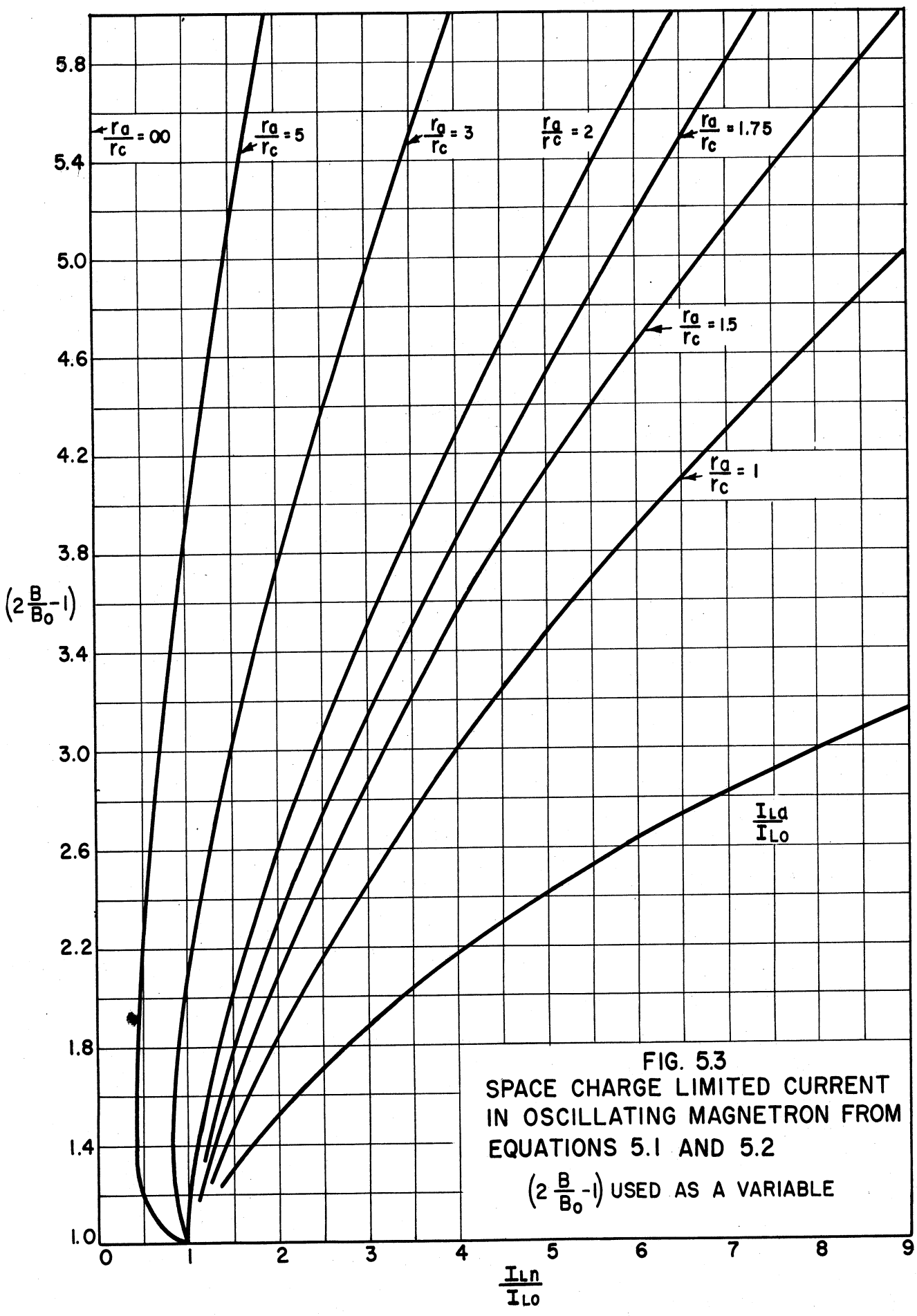

FIG. 5.3
SPACE CHARGE LIMITED CURRENT IN OSCILLATING MAGNETRON FROM EQUATIONS 5.1 AND 5.2
$(2\frac{B}{B_0}-1)$ USED AS A VARIABLE

two following parametric equations derived from Equation 5.1, 5.2 and 5.9.

$$\frac{I_{Ln}}{I_{Lo}} = \frac{r_n^2}{r_a^2}\,\frac{\beta_a^2}{\beta_n^2} = \frac{\frac{r_n}{r_c}\,\beta_a^2}{\frac{r_a^2}{r_c}\,\beta_n^2} \qquad 5.11$$

$$\frac{B}{B_o}^2 = \frac{1 - \frac{r_c^2}{r_a^2}}{1 - \frac{r_c^2}{r_n^2}} \qquad 5.12$$

In Figure 5.2 $\frac{I_{Ln}}{I_{Lo}}$ is plotted as a function of $\frac{B}{B_o}^2$ for various values of r_a/r_c.

In the oscillating magnetron the operating voltage is approximately given by the Hartree relationship

$$\frac{E_a}{E_o} = 2\,\frac{B}{B_o} - 1 \qquad 5.13$$

In Figure 5.3 the values of I_{Ln}/I_{Lo} are plotted as a function of $2\,\frac{B}{B_o} - 1$ to give an idea of the appearance of the maximum current boundaries on a performance chart. It must be kept in mind that the actual maximum current boundary is given by $\alpha_n\, I_{Ln}$ or about 0.71 the values given by the curves.

No experimental data have been examined yet to check these results. However, the current given are somewhat less than the one-half Allis current empirically determined

by Slater. The Allis current divided by α_a is plotted on the same scale for reference in both figures.

$$\left(\frac{I_{La}}{I_{Lo}} = \frac{1}{\alpha_a} \frac{I_{Aa}}{I_{Lo}} \right)$$

6. TEMPERATURE LIMITED OPERATION (H. W. Welch, Jr.)

The effect of temperature limited operation on maximum current boundary insofar as an actual limitation of available current is involved is fairly obvious. There are other effects observed experimentally, however, and the purpose of this section is to mention these briefly and point out through a simple qualitative analysis that other effects are to be expected.

The observed effects are briefly the following:

a. Starting voltage may change as temperature is reduced. This can be an increase or a decrease of 20 or 30 per cent in starting voltage. Changes have been observed in an increasing direction on the Model 6 f-m magnetron.

b. Maximum current boundary does not necessarily increase as temperature increases but in some cases may even decrease.

c. For a given temperature, maximum current boundary is dependent on magnetic field and loading. When temperature is changed the current boundary will have a new value still dependent on magnetic field and loading.

The first of these effects has been observed in this laboratory on a Model 6 magnetron operating at 13

centimeters. Unfortunately the tube failed before quantitative measurements could be made. Dr. Wilbur, of General Electric Laboratories, has also observed this effect in his tubes in the range below 1000 megacycles.

The second and third type of phenomena are clearly illustrated by the curves of Figures 6.1, 6.2 and 6.3, which are selected as typical from data supplied by Mr. Dench of Raytheon. For a given temperature it is obvious that maximum current boundary is different for different magnetic fields and loads. This may mean that peak currents during the r-f cycle are dependent on loading and magnetic field. It also may be related to an actual change in the space charge configuration. The fact that this may be the case is suggested by reference to Figure 6.4. The curves in this figure apply to a static magnetron. The curve labelled E_1 represents the potential corresponding to zero radial velocity in a region where space charge exists in the magnetron. Therefore it must be the potential at the boundary of a space charge swarm where no current is crossing. It is given by the following equation

$$E_1 = \frac{B^2 e}{8m} r^2 \left(1 - \frac{r_c^2}{r^2}\right)^2 \qquad 6.1$$

The curve labelled E_2 is the logarithmic distribution which exists in a space charge free diode given by

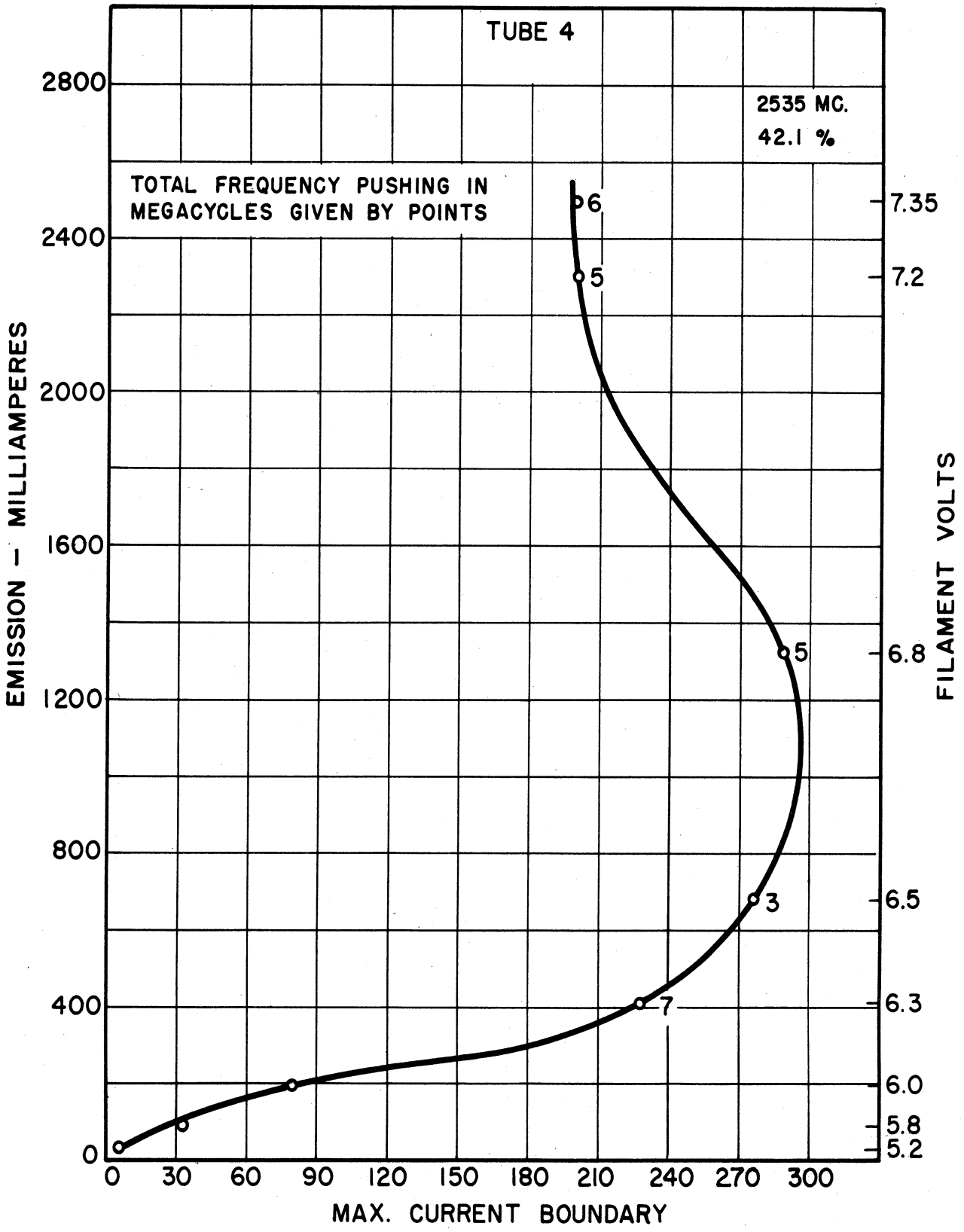

FIG. 6.1 EFFECT OF EMISSION ON MAXIMUM CURRENT BOUNDARY.- RAYTHEON DATA.

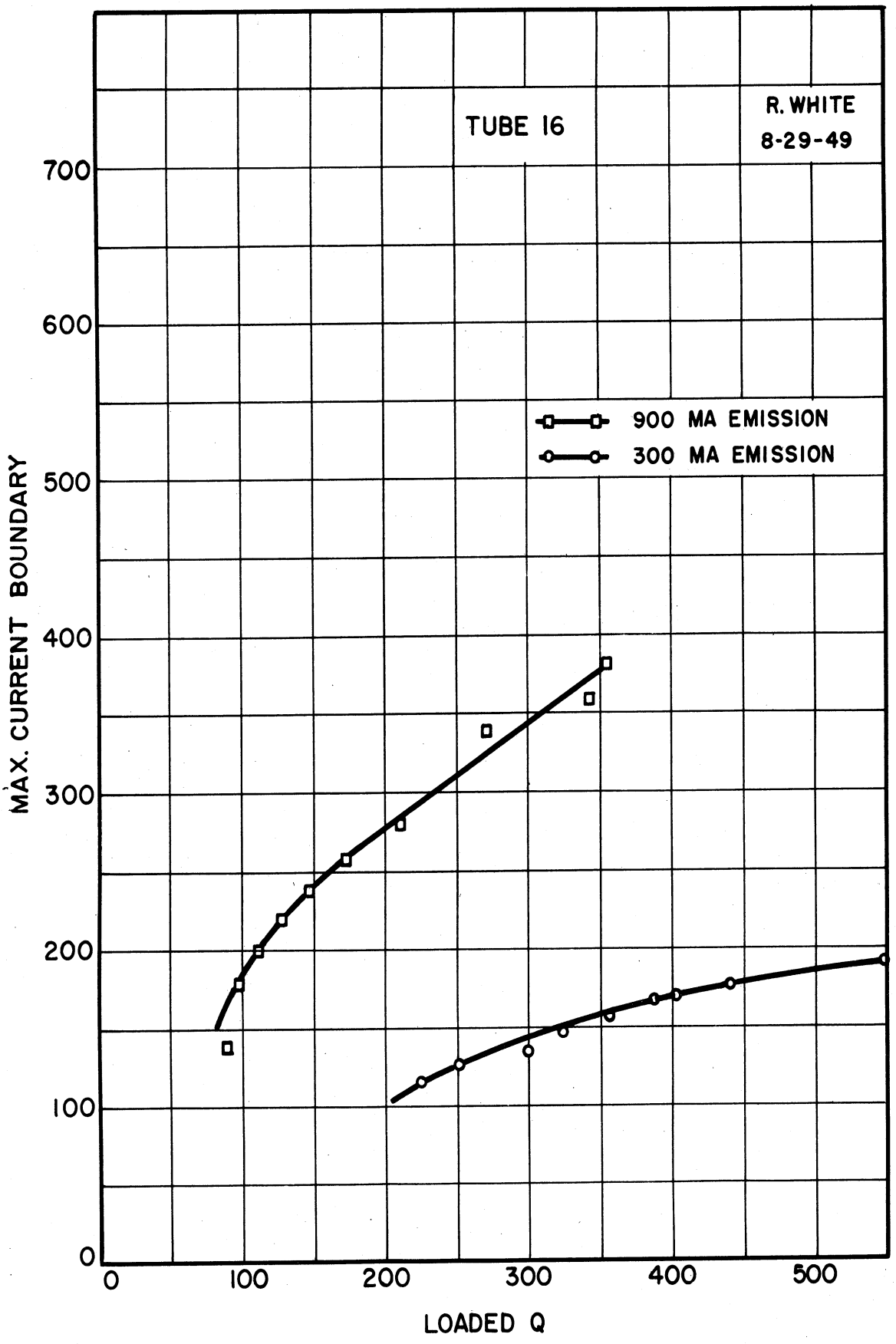

FIG. 6.2 EFFECTS OF LOADING ON MAXIMUM CURRENT BOUNDARY. RAYTHEON DATA.

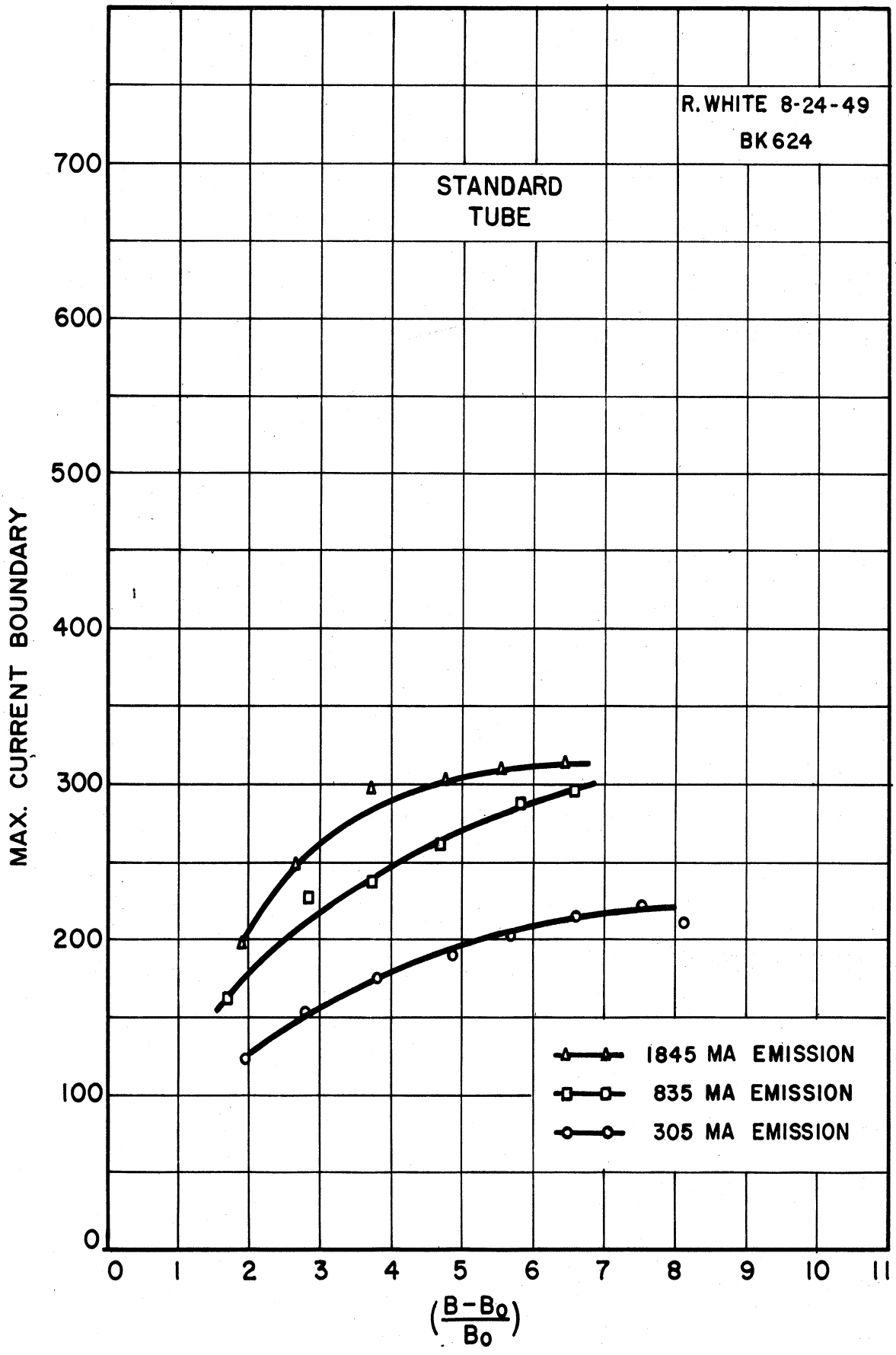

FIG. 6.3 EFFECT OF MAGNETIC FIELD ON MAXIMUM CURRENT BOUNDARY, RAYTHEON DATA

$$E_2 = E_a \frac{\log \frac{r}{r_c}}{\log \frac{r_a}{r_c}} \qquad 6.2$$

The curve labelled E_3 is the logarithmic curve which would exist in a magnetron between a boundary of the swarm r_H and the anode r_a if the anode potential were E_a. This curve is plotted from the following equation.

$$E_3 = B^2 \frac{e}{8m} r_H^2 \left[2 \left(1 - \frac{r_c}{r_H^2}\right) \log \frac{r}{r_H} + \left(1 - \frac{r_c^2}{r_H^2}\right) \right] \qquad 6.3$$

If we assume that the anode voltage applied is E_a it is apparent from these curves that under approximately space charge free conditions individual electrons would be found as far out as the radius r_T where they have no energy of radial motion and can therefore not cross the boundary. Between r_c and r_T individual electrons have everywhere energy of radial motion (therefore double stream radial current exists). This energy could be expressed by the difference in potential between the two curves, $E_2 - E_1$. On the other hand if space charge exists, and the region between r_c and r_H is filled with a swarm of electrons moving about the cathode, the distribution will be that given by Curve No. 3 and the electrons will only reach the boundary r_H. Intermediate conditions are, of course, conceivable. Curves 1 and 3 represent the extreme possibilities. The important point to be made in this discussion is that the extent of

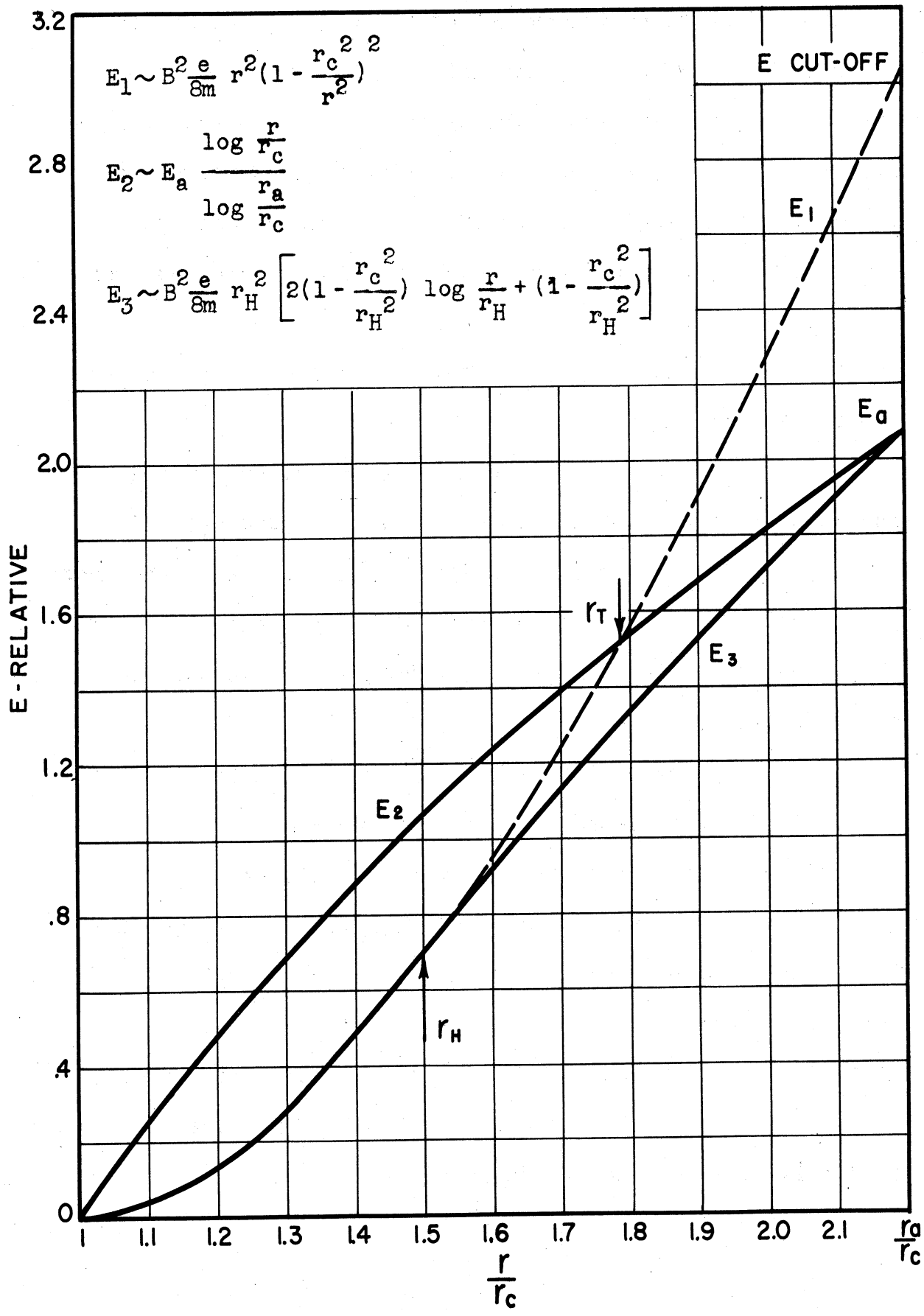

FIG. 6.4 COMPARISON OF SPACE CHARGE FREE AND MAGNETRON SPACE CHARGE CONDITION

the swarm depends on the amount of space charge within the swarm for a given anode potential.

By an extrapolation of these ideas to the oscillating magnetron in which current is being drawn through the swarm, it is apparent that under a condition of cathode saturation the smaller space charge density within the swarm could affect the following:

(a) The anode potential required for a given swarm configuration;

(b) The radial velocities of electrons through the swarm, therefore transit time and effect of loading;

(c) The average density of the swarm and, therefore, magnitude of rotating current and, possibly, penetration of electromagnetic field. These factors are also related to magnetic field.

Such an extrapolation has some validity since a relatively small increase in potential must exist at the edge of the swarm to account for the radial current. In conclusion, this qualitative discussion shows only that a relationship between maximum current boundary, available temperature limited emission, starting voltage, loading and magnetic field is to be expected. It is hoped that it will be possible to formulate a more quantitative picture, and this will be attempted in the immediate future.

7. LOW POWER MAGNETRON FOR LOW Q OPERATION (J. S. Needle)

In order to achieve more flexibility in the experimental program for study of low Q operation and at the same time to develop a tube usable in this type of operation at microwave frequencies, the construction of a low power magnetron to be used with an external cavity is being attempted. A sketch of this tube is shown in Figure 7.1. Only the capacitive portion of the resonant circuit is incorporated in the glass envelope. The tube will be called Model 9. Except for the radiation shield and by-pass condensor, discussion of which is forthcoming, the design has been completed and construction is under way.

There are two very desirable features inherent in the Model 9 magnetron which are valuable for the study of magnetron behavior; (a) the size and shape of the oscillator cavity can be easily changed, and (b) the two halves of the anode structure may be operated at different d-c potentials. The flexibility of this structure suggests possibilities in its application to the work now in progress at the University of Michigan. The applications which are presently envisioned for this tube are listed below:

a) A tool for a study of effect of loading on maximum current boundary and pushing.

b) To serve for the investigation of the optimum impedance for higher power coaxial line oscillator cavity.

c) To provide information as to the possibility

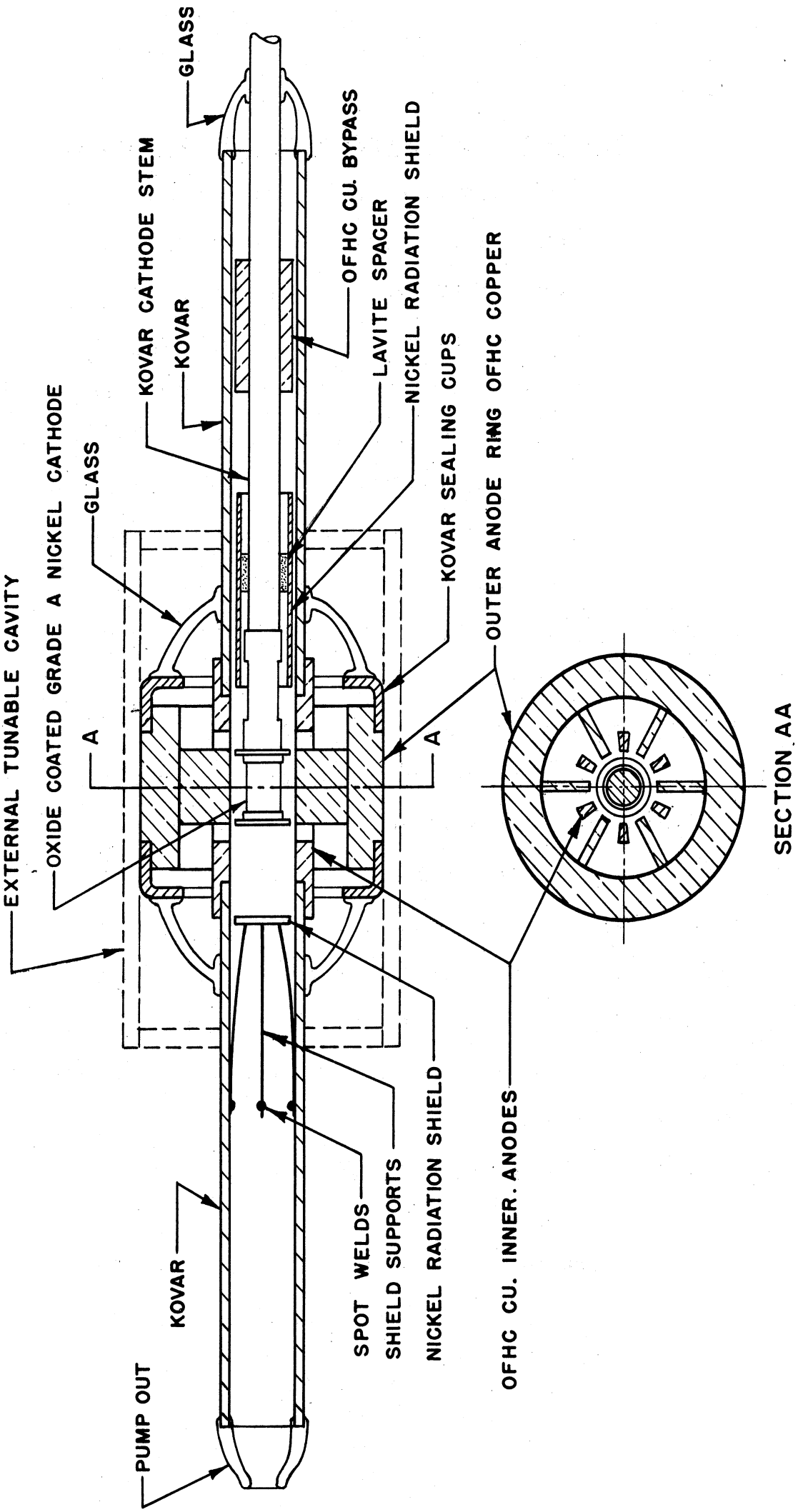

FIG. 7.1 SKETCH OF LOW POWER MAGNETRON
FOR USE IN EXTERNAL TUNABLE CAVITY

of frequency modulating the oscillator by employing a variable voltage on one set of anodes with respect to the other (see G.E. Report No. R.L. 341, April, 1950).

d) To serve as a more adequate (2 - 10 watt) signal generator in our measurement laboratory, and to provide a prototype for other low power applications such as local oscillators.

e) To provide design experience for the construction of higher power ceramic seal tubes of similar geometry.

The evacuated portion of the Model 9 magnetron consists of a 12-anode coaxial structure and an oxide-coated cathode. A magnetic field of approximately 1600 gauss will be supplied by a solenoid. The proximity of the inner to outer anode glass seals to the emitting region of the cathode necessitates the use of radiation shields. These shields, due to their fixed geometry and position, will result in a frequency sensitive cathode line. Tests on the Model 7 magnetron, as discussed in section 10 of this report emphasize the need for a heavy cathode by-pass condensor in order to prevent power loss through the cathode line. The design of the radiation shields and the cathode by-pass as well as the relative placement of these elements along the cathode line will be based on the results of a series of cold tests to be run before final assembly. The quantities listed below have entered into the design of the Model 9 magnetron.

λ = 10 cm
$n\lambda$ = 60
n = N/2 = 6
r_a = 0.125 in.
r_c = 0.76 in.

$\frac{r_a}{r_c}$ = 1.66

E_o = 280 volts
E = 1400 volts
B_o = 554 gauss
B = 1662 gauss
vane height = 0.25 in.

8. EXPERIMENT ON D.C. MAGNETRON (W. Peterson)

The major purpose of this experiment is to attain a more complete understanding of the magnetron by studying the space charge in a smooth bore d-c magnetron. Some theoretical work has been done to explain the nature of space charge, but it is felt that experimental verification of the theories is lacking. Such experimental work, along with similar work done in other laboratories, can, it is hoped, serve to integrate the various theories and make the understanding of magnetron space charge more vivid.

Regner Svensson, Stockholm, Sweden, has recently carried out some experiments, sending a beam of electrons through a magnetron, with moderate success. Work on d-c magnetrons also has been done at the Bureau of Standards by Reverdin and Marton. The results will be presented at the Mexico Meeting of the American Physical Society in June, 1950. A project is being undertaken by Lamb and Nedderman at Columbia University to measure the space charge density in a magnetron by a unique method. A beam of helium atoms

is to be injected into the space charge, and the number of atoms excited to certain metastable states will be measured.

The quantities of interest in such experiments are the potential distribution, the space charge density, the electron orbits, and perhaps the electron velocities. Given any one of these four quantities, all the others can be calculated. The relation between potential distribution and space charge density is, of course, Poisson's equation. Obviously the electron orbits can be found from the velocities by integration. Usually in theory initial velocities are neglected; in this case one can use the relationship resulting from conservation of angular momentum, which gives the angular velocity as a function of the radius for any electron.[1] Given the angular velocity and the orbit, the radial velocity and total velocity can be found, since the total velocity at any point has the direction of the tangent to the orbit at that point. Finally, if the velocities are known, the potential can be found by the law of conservation of energy, i.e. $E = \frac{1}{2}\frac{m}{e}V^2 + E_{cathode}$. Also, with the potential known, the magnitude of the velocity can be found. From this and the angular component, the direction and radial component can be determined. Furthermore, the radial current, $I_r = 2\pi r \rho V_r$, must be constant; this gives a simple relation between velocity and space charge density.

Now the question arises: what shall we measure?

---

1 See Equation 5.5, Technical Report No. 1, for example.

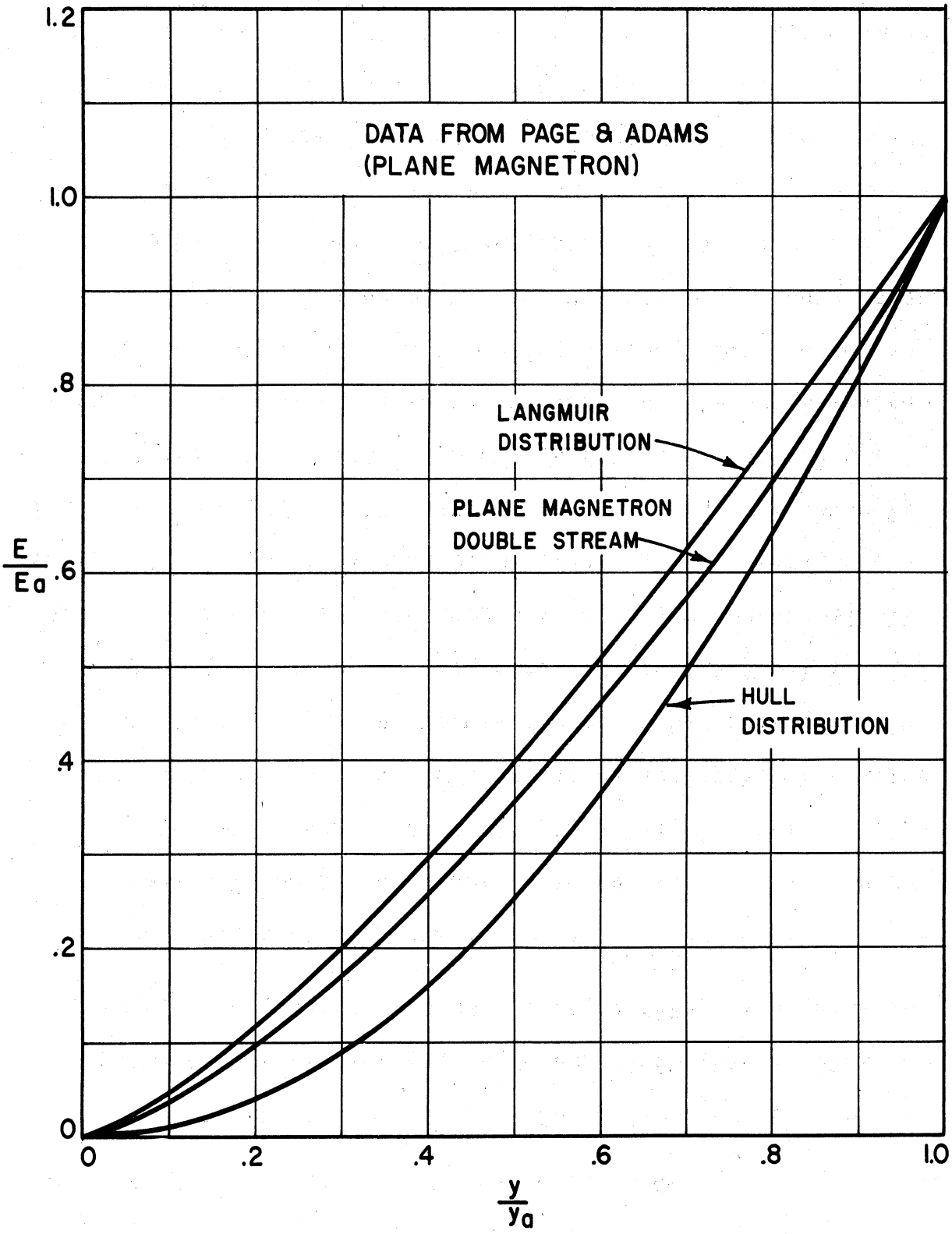

FIG. 8.1 POTENTIAL DISTRIBUTION IN PLANE DIODES

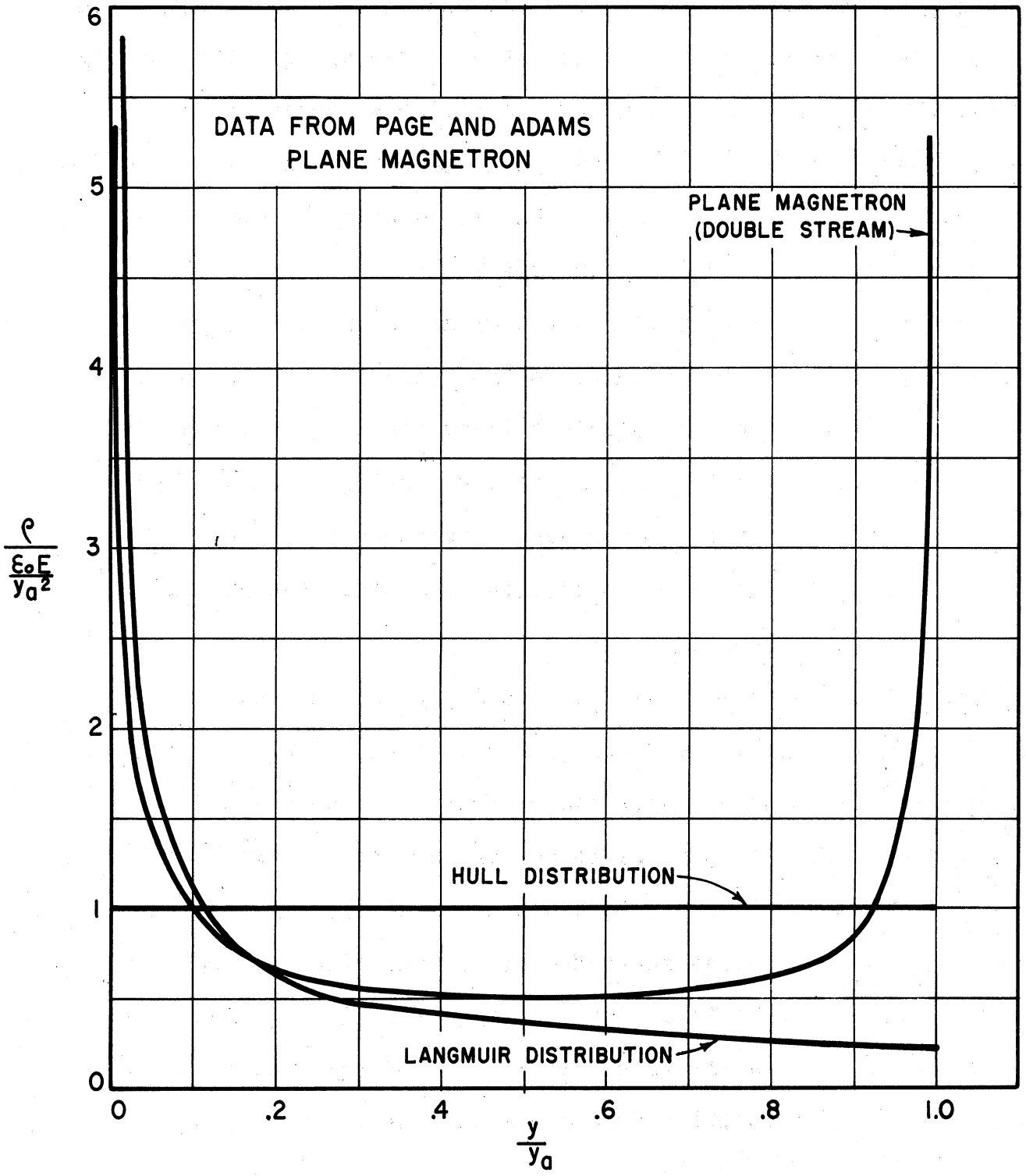

FIG. 8.2 SPACE CHARGE DISTRIBUTION IN PLANE DIODES

In general, errors become more pronounced upon differentiation, and less pronounced upon integration. One can see this easily if one compares the potential distribution curves for an ordinary plane diode, for the plane magnetron as Slater found it, and for the plane case of Hull's solution. They are very similar, while the orbits and space charge are radically different. The orbits for the ordinary plane diode are straight lines perpendicular to the cathode, whereas in the Hull solution they are straight lines parallel to the cathode. The "double-stream" solution has cycloid-like orbits. The potential distributions and space charge densities are shown in Figures 8.1 and 8.2, respectively.[1] Since the potential must be differentiated to find the space charge density, and since space charge density is usually found indirectly by measuring potential and using Poisson's Equation, it seems preferable to avoid these two as quantities to measure.

What we propose to measure is the electron position as a function of time. This yields almost immediately the other two quantities mentioned, i.e., the electron orbit and the electron velocity. The electron orbit is of course just the locus of the electron's position; for the electron velocity, the position function must, unfortunately, be

---

1 Most of this data was taken from a concise article, "Space Charge in Plane Magnetron", L. Page and N. I. Adams, Physical Review, V69, page 492.

differentiated. The expression for conservation of angular momentum also can be used to obtain the electron velocity from the orbit, in order to check our work. The potential and space charge density can be found by using the simple algebraic formulas, $E = E_{cathode} + \frac{1}{2}\frac{m\,v^2}{e}$, and $\rho = \frac{j}{2\pi r v_r}$, the results of which will have errors of the same order of magnitude as the errors in our original experimental measurements.

A tube for this work is now being designed. It will be a d-c smooth bore magnetron with an electron gun in the same envelope. The gun will introduce a beam of electrons in an axial direction tangent to the cathode at one end of the tube. The electron beam leaving the space charge at the other end will strike a fluorescent screen. Presumably these electrons will have the same motion as electrons emitted from the cathode except for the added axial component of velocity. To find where an electron will be T seconds after it is emitted, one adjusts the beam velocity so that the beam electrons spend time t in the space charge. The radial and axial displacement of the beam while traveling through the tube will presumably be the same as the displacement of the emitted electron.

This method has the advantage of measuring the electron orbits directly and allowing us to compute in a simple manner the other quantities of interest without interfering with the magnetron's operation during measurement.

It seems worth mentioning that this method may have applications beyond this simple experiment. It is hoped that eventually it amy be used on oscillating magnetrons to find orbits in a case defying any analytical procedure.

The first consideration in designing the tube was size. A tube as small as the average magnetron would have orbits too small to measure on any fluorescent screen; while a large tube would require prohibitive voltages. In a short tube, end effects would be large; while a long tube would require excessive current. We chose to start our work with a diode having an anode two inches in diameter and a cathode one-half inch in diameter and two inches long.

The beam voltage is somewhat limited. A conventional gun can be operated over a range of voltages of perhaps 5:1. This gives a range of about 2.3:1 in beam velocity, or in the time the beam electrons spend in the space charge. Thus, we can see only a portion of the orbit in any one set of operating conditions.

The electrons, according to theory, travel in cycloid-like paths with one loop taking approximately $\frac{2\pi}{\omega_L}$ seconds. Now when the tube length and beam voltage range are determined, the range of time the beam spends in the space charge is determined, of course. Then we must choose ω_L (which amounts to choosing B) properly to see any particular part of the orbit. Fortunately, the required fields are easy to obtain. For example, for a tube two inches

long and with a 500-volt electron beam, B should be approximately 200 gauss for one loop.

Probably our biggest problem will be the placement of the fluorescent screen. The screen must be near the space charge, because the electron beam will not have an axial direction after leaving the space charge. Even then the beam must travel in a magnetic field. At this point two problems arise: first, the fluorescent screen must be able to stand the heat from the cathode; and second, the stray electrons from the space charge which strike the screen must not destroy it and must not obliterate the beam spot. We hope that the screen can be placed close enough to the space charge so that with only first order corrections, we will have fairly accurate results.

9. R-F PROPERTIES OF MAGNETRON SPACE CHARGE (G. R. Brewer)

A. Propagation of electromagnetic waves in a magnetron space charge--theoretical analysis. The propagation of electromagnetic waves in an ionized media has been treated in a large number of papers, particularly with reference to the ionosphere. However, only a very small number of these papers[1] are even approximately applicable to the type of

---

1 Technical Report No. 1, H. W. Welch, Jr.
"High Frequency Behavior of a Space Charge Rotating in a Magnetic Field", Physical Review, V57, J. P. Blewett and S. Ramo, page 635-641, April, 1940.
"Space Charge Frequency Dependence of a Magnetron Cavity", W. E. Lamb and M. Phillips, Journal of Applied Physics, V18, page 230-238, Feb. 1947.

space charge region which exists in a magnetron.

It is well known that the problem of the interaction between the fields in a multi-anode magnetron and the rotating space charge cloud is sufficiently complex to have allowed, to date, only solutions containing several restrictive approximations. This analysis is therefore concerned with the interaction of electrons in a specified space charge cloud with certain uniform and simple types of electromagnetic fields. It is believed that the results will be applicable in the case of space charge clouds used for frequency modulation, which are usually placed in a structure of such geometry that the simple field analysis is valid. It is also hoped that from these results one may be able to deduce qualitatively or semi-quantitatively the effects in the case of the more complicated fields of a multi-anode magnetron.

This analysis is a continuation of that reported in Technical Report No. 1 and is an attempt to determine the effective index of refraction of the space charge region as seen by an electromagnetic wave propagating into or through the medium. A knowledge of the index of refraction, and thus the dielectric constant, as a function of the frequency of the wave, and the magnetic field, will enable the calculation of the reactive (and in some cases also resistive) effects of the space charge on the microwave circuit.

In Technical Report No. 1 this problem was treated under the assumption that the space charge swarm is moving

with constant velocity and perpendicular to the electron motion so that the second term on the left side of Equation 9.1 below was not included. The present work is a refinement on the previous treatment in that the variation in the electron velocity with position in the magnetron is included.

In order to simplify the mathematics involved, two limiting cases are chosen: that of the plane magnetron, and the cylindrical magnetron with small cathode. We will outline below the method of analysis used and the results obtained to date; it is planned to include this material in detail together with results of experimental investigations of the r-f properties of the space charge cloud in a future technical report.

In the analysis to follow we make the following assumptions:

(a) For the purposes of this analysis the space charge is considered as an isothermal free electron gas of determined density.

(b) The angular velocity and the charge density is given by the Hull-Brillouin relations (Equations 9.3 and 9.8 below).

(c) For the cylindrical case $r_c^2/r_a^2 \ll 1$.

(d) The linear electron velocities are small enough that a non-relativistic treatment will be valid.

Then the Euler hydrodynamical equation governing the electron motion can be written

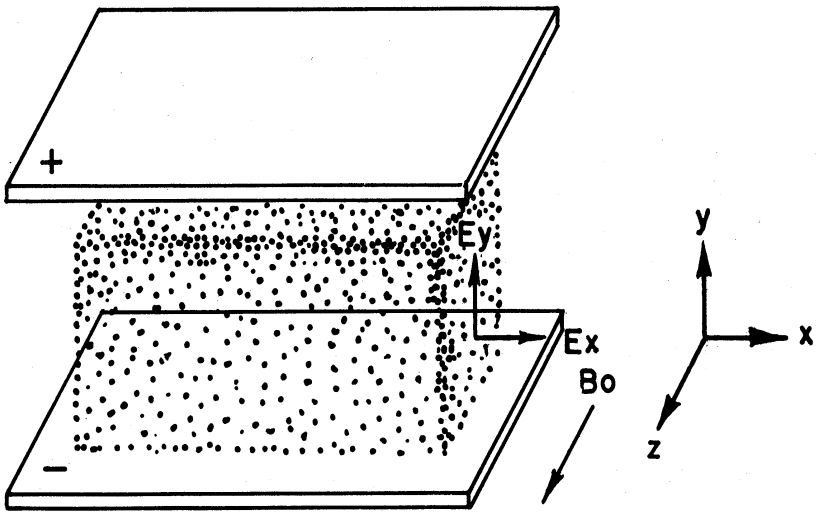

FIG 9.1 COORDINATE SYSTEM AND FIELD VECTORS OF PLANE MAGNETRON

$$\frac{\partial \vec{v}}{\partial t} + (\vec{v} \cdot \nabla)\vec{v} = -\frac{e}{m}\left[\vec{E} + \vec{v} \times \vec{B}_o\right] - \frac{e}{m\rho}\nabla p \qquad 9.1$$

Writing for the gas pressure $p = \frac{\rho}{e} k T$, under our assumption of an isothermal gas the last term becomes $-\frac{k T}{m\rho}\nabla\rho$ which vanishes under our assumption of a constant space charge density. In the above equation

$\vec{v}$ = linear velocity of a group of electrons contained in volume $d\tau$

B_o = constant +z directed applied magnetic field

ρ = space charge density

T = electron gas temperature

k = Boltzmann's constant .

In order to separate the equations into steady or d-c and fluctuating or high frequency parts we consider the velocity and electric field to be made up of a steady term and a perturbation term.

$$\vec{E} = \vec{E}_o + \vec{E}_1$$

$$\vec{v} = \vec{v}_o + \vec{v}_1$$

And to linearize the equations we shall neglect products of two perturbation terms.

Then the fluctuating part of Equation 9.1 becomes

$$\frac{\partial \vec{v}_1}{\partial t} + (\vec{v}_1 \cdot \vec{\nabla})\vec{v}_o + (\vec{v}_o \cdot \vec{\nabla})\vec{v}_1 = -\frac{e}{m}\left[\vec{E}_1 + \vec{v}_1 \times \vec{B}_o\right] \qquad 9.2$$

In the above we have tacitly supposed the charge density to be constant so that

$$\nabla\cdot(\rho\vec{v}) = -\frac{d\rho}{dt} = -\frac{\partial\rho}{\partial t}$$

This will be valid if the charge density does not change appreciably within a volume whose dimensions are small compared with a wavelength of the r-f wave being propagated in the gas.

1. Plane magnetron. From assumption (b) above, the space charge is determined by the following equations:

$$\begin{aligned} E_o &= -\omega_c By \\ v_o &= -\omega_c y \\ \rho &= -\varepsilon_o \frac{m}{e}\omega_c^2 \\ \omega_c &= \frac{eB}{m} \end{aligned} \qquad 9.3$$

Figure 9.1 shows the field vectors and coordinate system for the plane magnetron case.

We shall consider wave propagation normal to the applied magnetic field, in the x and y directions; propagation in the z direction yielding the same results as that in the y direction. The propagated wave will have field components E_x E_y H_z; an electric field in the direction of the applied magnetic field will produce electron motions yielding the well-known value of dielectric constant for an ionized region, dependent only on the space charge density,

independent of the method of production of this space charge and is therefore relatively uninteresting for the purposes of this analysis.

a. Wave propagation in +y direction. The perturbed velocity and field quantities are allowed to vary as $e^{i\omega t - \gamma y}$. Then substitution of 9.3 into 9.2, together with the field equations

$$\nabla \times H_1 = \rho_o v_1 + i\omega \varepsilon_o E_1$$

$$\nabla \times E_1 = - i\omega\mu_o H_1 \qquad 9.4$$

allows the solution for γ for the plane wave ($\partial/\partial x = 0$, $v_z = 0$)

$$\gamma^2 = \frac{\omega_c^2 - \omega^2}{c^2} \qquad 9.5$$

where c is the velocity of light and $\omega = 2\pi f$ where f is the frequency of the propagating wave. Since γ^2 can be either positive or negative depending on the relative values of ω_c and ω, we must conclude that γ is imaginary and let

$$\gamma = \frac{i\omega}{v} = \frac{i\omega\eta}{c}$$

η is the index of refraction of the charged region and in this case is real so that $\eta^2 = \varepsilon_{eff}$. From 9.5

$$\varepsilon_{eff} = 1 - \frac{1}{(\omega/\omega_c)^2} \qquad 9.6$$

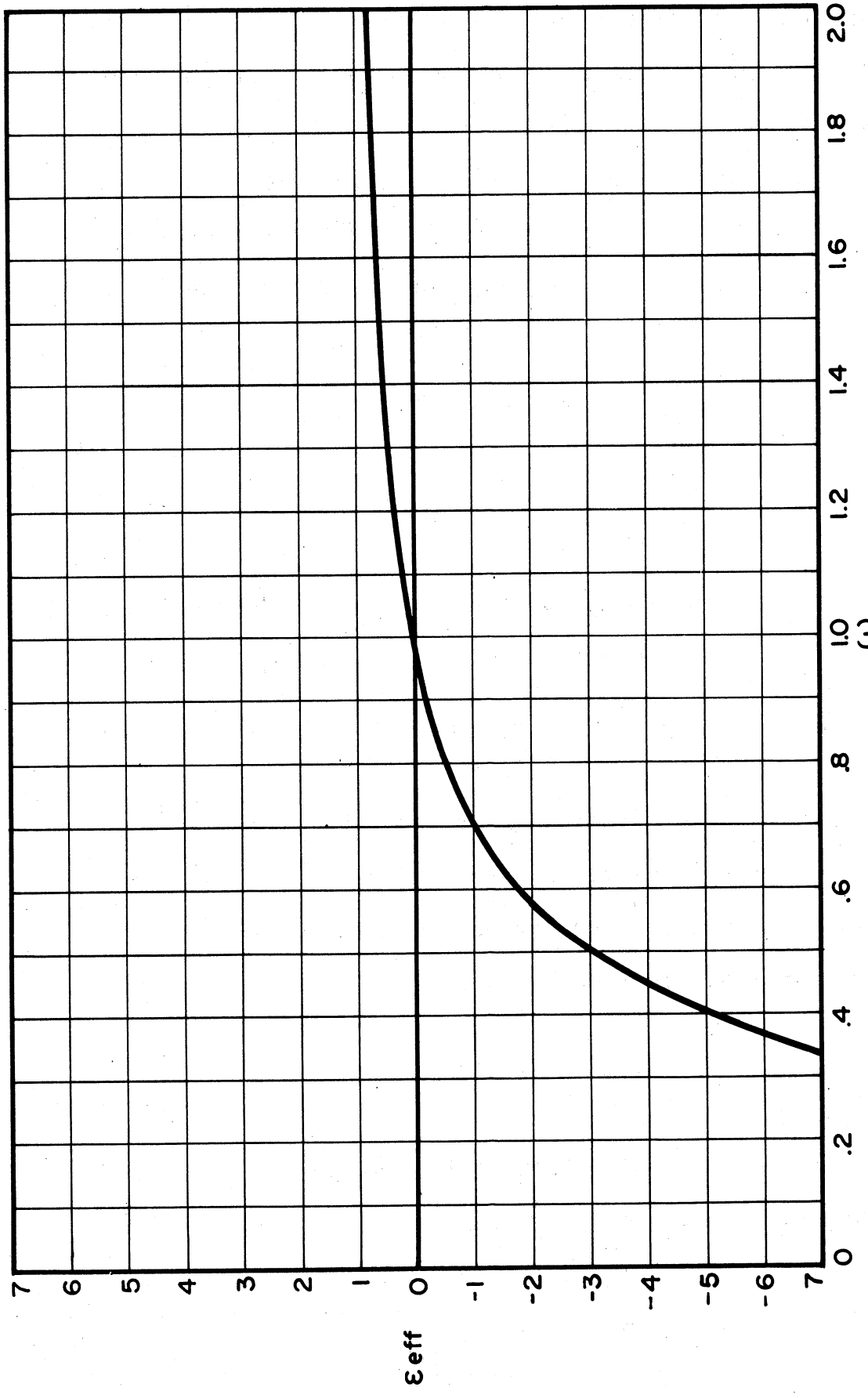

FIG. 9.2 εeff FOR PLANE MAGNETRON
PROPAGATION NORMAL TO MAGNETIC FIELD

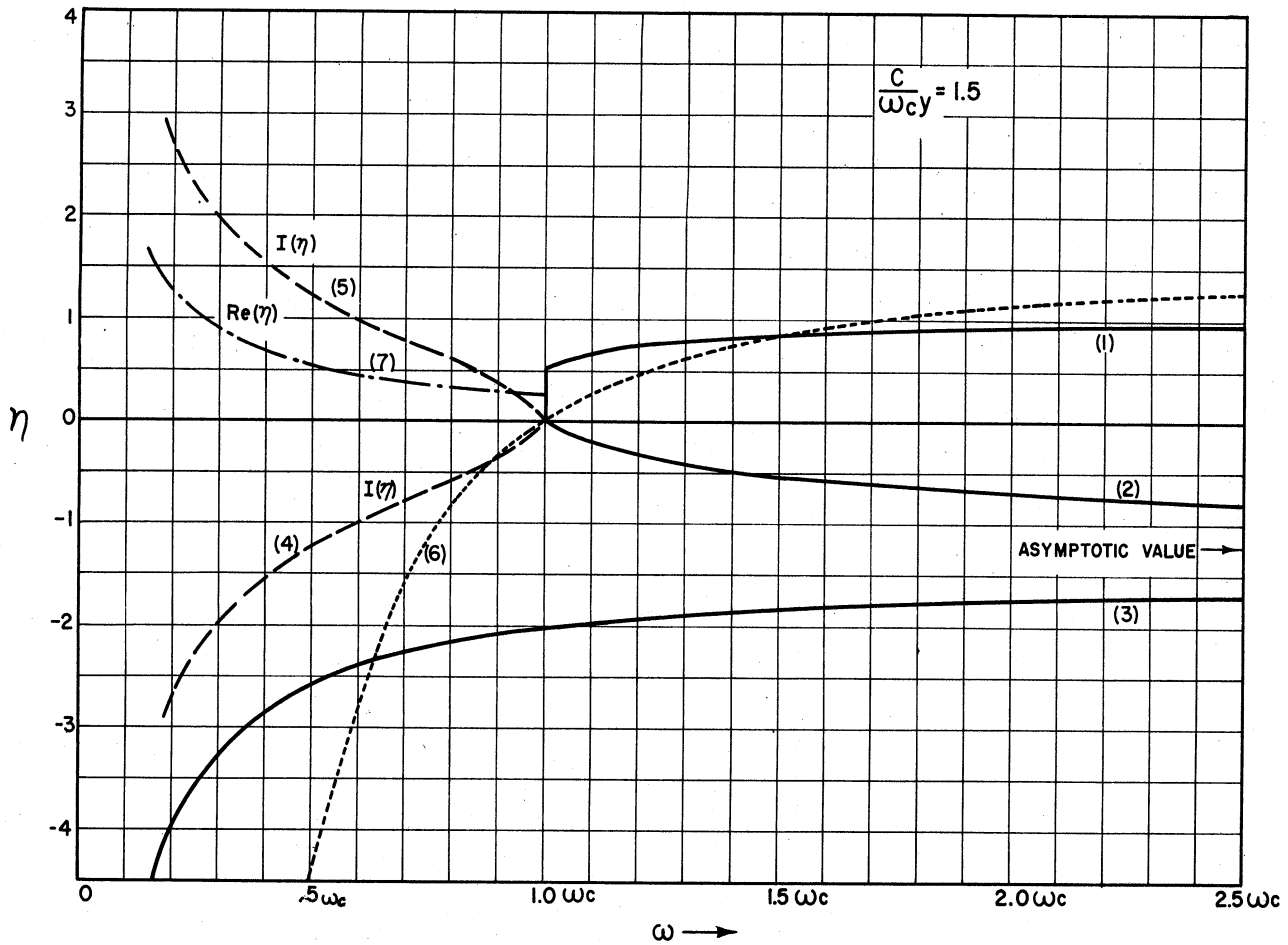

FIG. 9.3a INDEX OF REFRACTION OF PLANE MAGNETRON
PROPAGATION IN ± Z DIRECTION

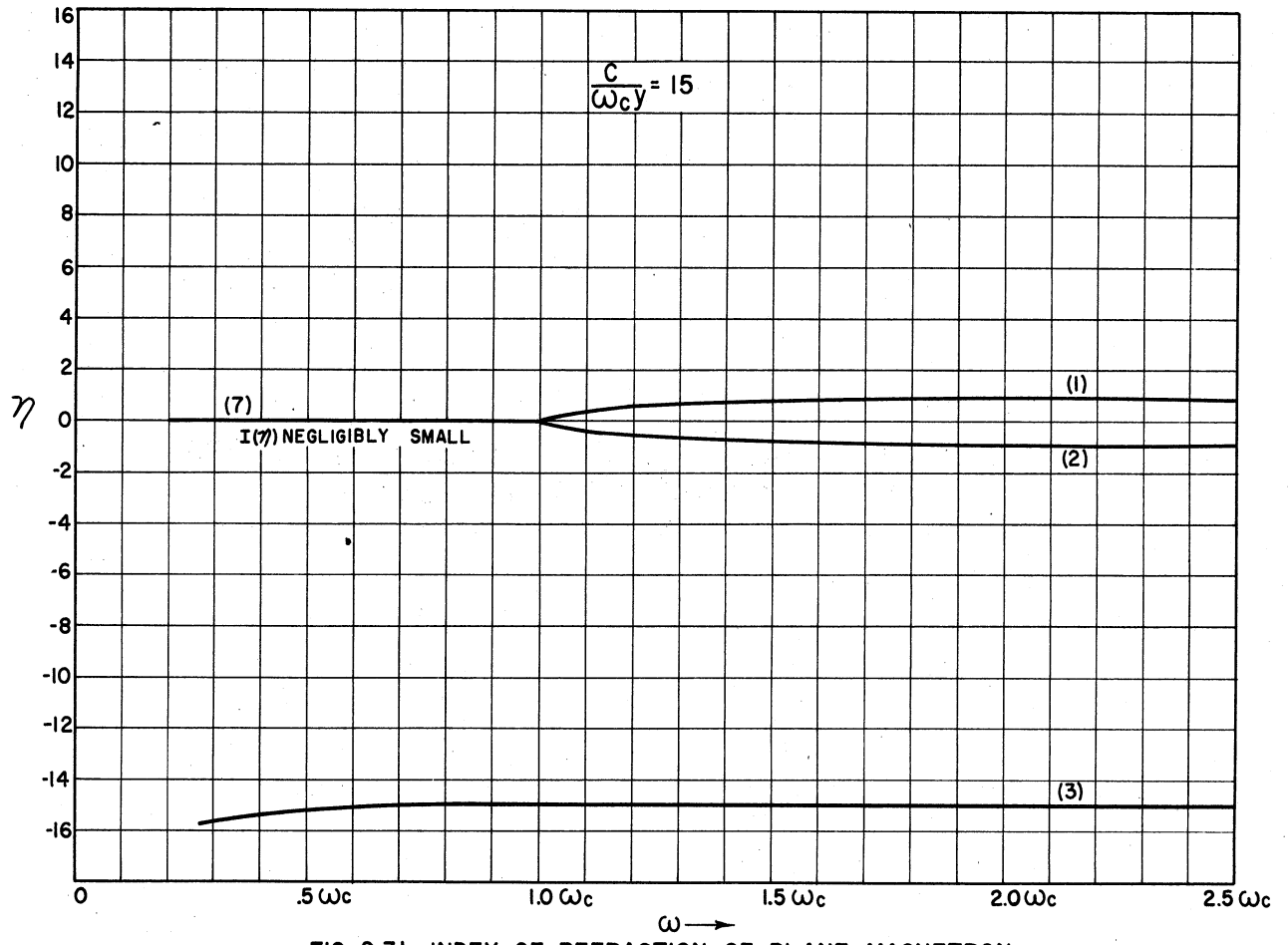

FIG. 9.3b INDEX OF REFRACTION OF PLANE MAGNETRON
PROPOGATION IN ± Z DIRECTION

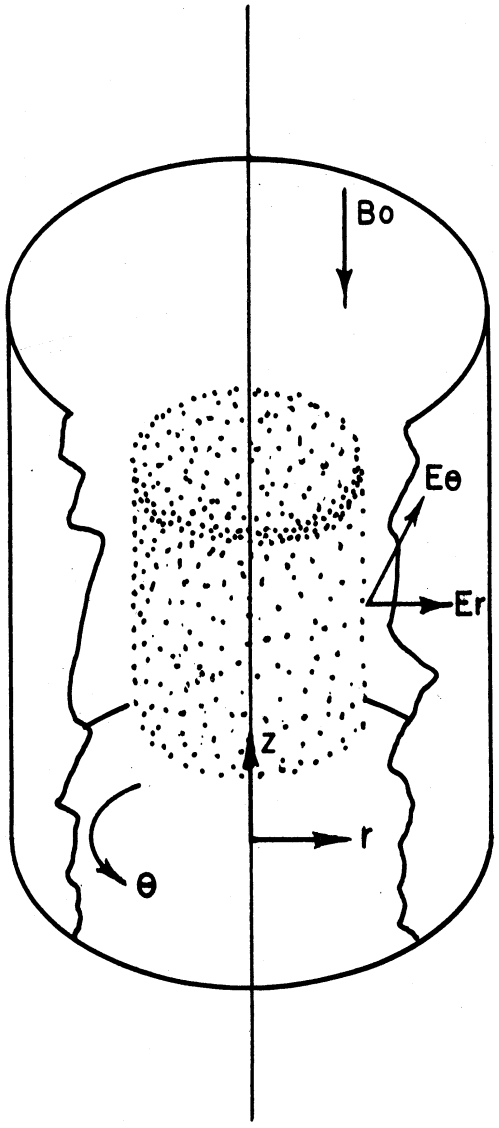

FIG. 9.4 COORDINATE SYSTEM AND FIELD VECTORS OF CYLINDRICAL MAGNETRON

Since γ appears only as a square, the same value of $\mathcal{E}_{eff}$ will result from consideration of a wave propagated in the -y direction. Equation 9.6 is plotted in Figure 9.2.

b. Propagation in the x direction. In this case all perturbed quantities are considered to vary as $e^{i\omega t - \gamma x}$ and the propagated wave to possess field components E_x E_y H_z. Then, as before, a combination of equations (9.2, 9.3, and 9.4) allow a solution for the propagation constant in the two relations

$$\gamma = \frac{i}{y}\frac{\omega}{\omega_c}\left(1 - \frac{1}{(\omega/\omega_c)^2}\right)$$

$$\gamma^3 + \frac{i\omega}{\omega_c y}\gamma^2 + \frac{\omega^2}{c^2}\gamma + \frac{i\omega^3}{c^2\omega_c y}\left(1 - \frac{1}{(\omega/\omega_c)^2}\right) = 0$$

Substituting $\gamma = \frac{i\omega\eta}{c}$ and $\eta^2 = \mathcal{E}_{eff}$ these become:

for the first: $$\mathcal{E}_{eff} = \left[\frac{c}{\omega_c y}\left(1 - \frac{1}{(\omega/\omega_c)^2}\right)\right]^2 \qquad 9.7$$

for the second: $$\eta^3 + \frac{c}{\omega_c y}\eta^2 - \eta - \frac{c}{\omega_c y}\left(1 - \frac{1}{(\omega/\omega_c)^2}\right) = 0$$

These equations are plotted in Figures 9.3 and 9.4 for two values of $\frac{c}{\omega_c y}$.

Examination of Figure 9.3 for the case $\frac{c}{\omega_c y} = 1.5$ (the non-relativistic treatment is only a rough approximation for values of $\frac{c}{\omega_c y}$ less than about 2.5) yields several interesting

facts.

(a) The frequency scale is divided by the cyclotron frequency ω_c into two rather distinct regions; that for $\omega < \omega_c$ and for $\omega > \omega_c$.

(b) In both of these regions there can exist four separate waves. For $\omega > \omega_c$ these waves travel without attenuation but for $\omega < \omega_c$ the index of refraction η is complex $\eta = R_e(\eta) + i\, I(\eta)$ for two of the wave so that for these the wave amplitude can change.

(c) In the region $\omega > \omega_c$ two of these waves (2,3) travel with the electron motion ($\eta < 0$) and two (1,6) against their motion ($\eta > 0$). None of these waves are attenuated, but the phase velocity may exceed that of light.

(d) In the region $\omega < \omega_c$ two waves (7+5, 7+4) travel against the steady electron motion and two (3,6) with their motion. Of the former, one is attenuated and one increases in amplitude as it progresses through the space charge. This latter, of course, suggests the possibility of amplification by such an electron stream.

2. Cylindrical magnetron. In the cylindrical case the space charge cloud is assumed to be determined by the Hull-Brillouin relations:

$$\rho = -\frac{m}{e}\,\frac{\omega_c^2\,\varepsilon_o}{2}\left[1 + \left(\frac{r_c}{r}\right)^4\right] \qquad 9.8$$

$$\Omega = \frac{\omega_c}{2}\quad 1 - \left(\frac{r}{r_c}\right)^2$$

where Ω is the angular velocity of the electron rotating around the cathode.

We shall consider wave propagation parallel to and normal to the applied magnetic field. The propagated wave of interest will have field components E_r H_θ in the former case and E_θ H_z in the latter case.

a. Wave propagation in the z direction. In this case we consider the propagation of a TEM wave, field components E_r H_θ, along the coaxial line formed by the filamentary cathode and smooth cylindrical anode of a magnetron. Upon entering the space charge region the wave must have field components E_r E_θ H_θ H_r H_z. Thus, Equation 9.2 in component form becomes:

$$i\omega v_r = -\frac{e}{m} E_r - \omega_c v_\theta$$

$$i\omega v_\theta + v_r \frac{\partial v_o}{\partial r} = -\frac{e}{m} E_\theta + \omega_c v_r \qquad 9.9$$

Solving for the velocities and letting $v_o = r\Omega$ and $\xi = \frac{\omega_c}{2}\left[1 - \frac{r_c^2}{r^2}\right]$ the r-f currents are:

$$J_\theta = \rho v_\theta = -\frac{\rho \frac{e}{m}\left[E_r + i\frac{\omega}{\xi} E_\theta\right]}{\omega_c \xi - \omega^2}$$

$$J_r = \rho v_r = \frac{\rho \frac{e}{m}\left[E_\theta - i\frac{\omega}{\omega_c} E_r\right]}{\omega_c \xi - \omega^2} \qquad 9.10$$

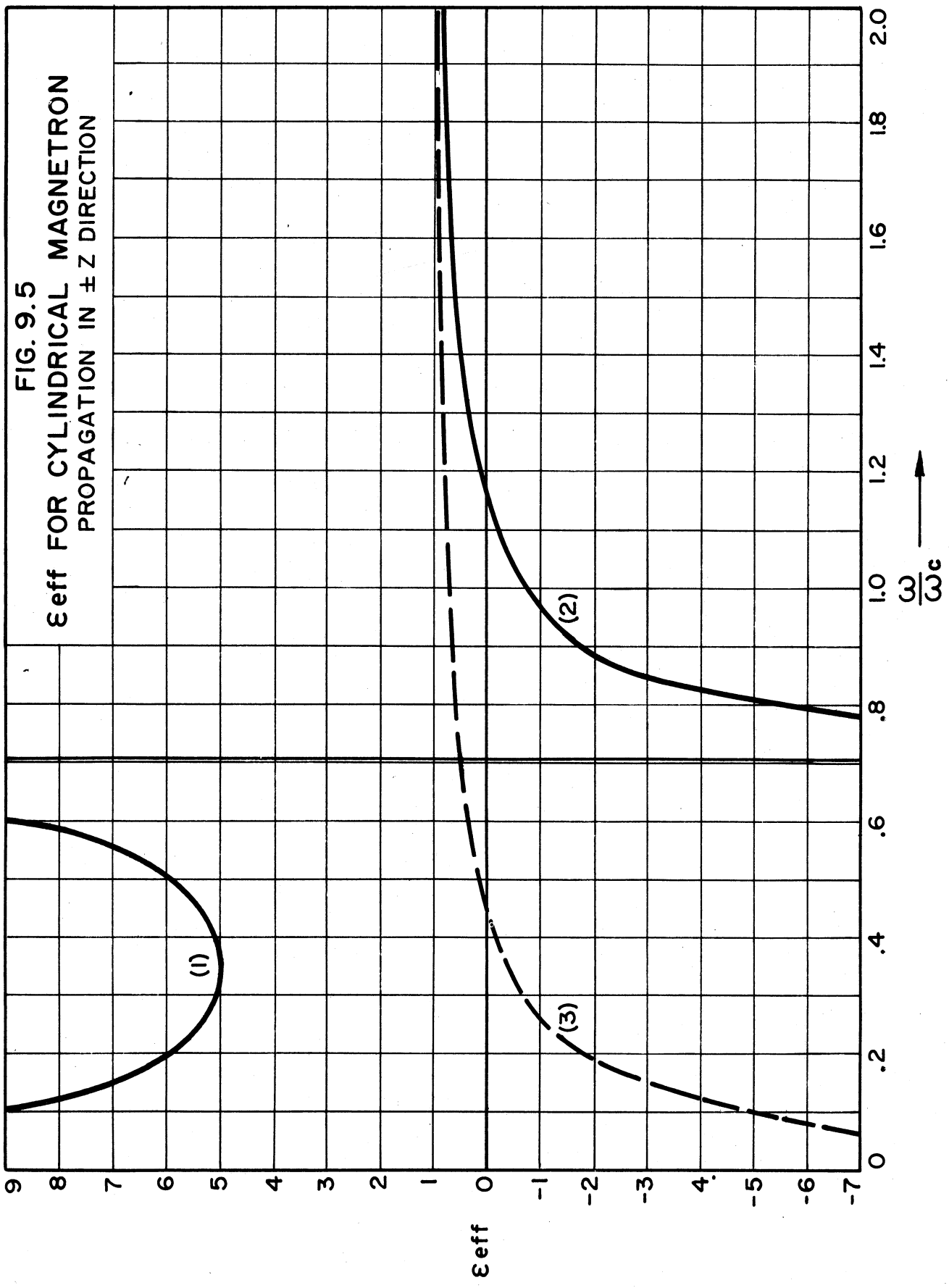
FIG. 9.5
εeff FOR CYLINDRICAL MAGNETRON
PROPAGATION IN ± Z DIRECTION
(1)
(2)
(3)
εeff
9 8 7 6 5 4 3 2 1 0 -1 -2 -3 -4 -5 -6 -7
0 .2 .4 .6 .8 1.0 1.2 1.4 1.6 1.8 2.0
ω/ωc

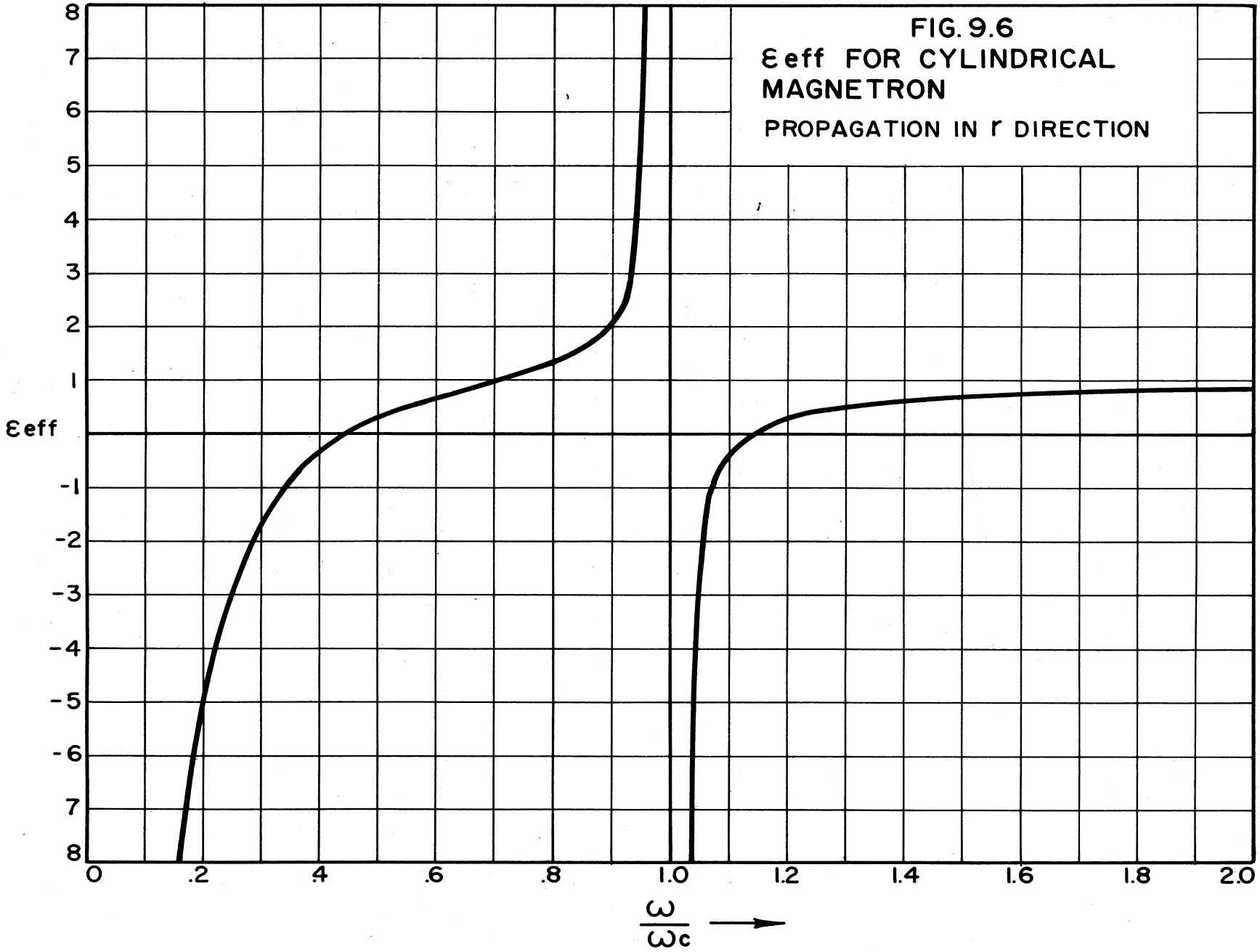
FIG. 9.6
εeff FOR CYLINDRICAL MAGNETRON
PROPAGATION IN r DIRECTION
εeff
8
7
6
5
4
3
2
1
-1
-2
-3
-4
-5
-6
7
8
0
.2
.4
.6
.8
1.0
1.2
1.4
1.6
1.8
2.0
ω/ωc

Substitution into the field equations (9.4) and simplification yields the following relation for the index of refraction.

$$\eta^2 = 1 - \frac{1 \pm \frac{1}{\sqrt{2}\frac{\omega}{\omega_c}}}{1 - 2\left(\frac{\omega}{\omega_c}\right)^2} \qquad 9.11$$

This equation is plotted in Figure 9.5, from which it is seen that there can exist two waves in the medium. For $\omega < \omega_c/\sqrt{2}$ one of these waves is characterized by an imaginary refractive index and so is attenuated. These curves are seen to be similar to those presented in Technical Report No. 1, Figure 19b.

b. Propagation in the r direction. The field components in the space charge are the same in this case as in the previous section, E_r, E_θ, H_θ, H_z. Then the r-f currents are as given by Equations 9.9 and substitution in the field equations yields the following relation for the effective dielectric constant, subject to the conditions $\partial/\partial z = \partial/\partial\theta = 0$ for all perturbation quantities.

$$\varepsilon_{eff} = 1 - \frac{1}{4} \frac{1}{\left(\frac{\omega}{\omega_c}\right)^2} \frac{1 - 2\left(\frac{\omega}{\omega_c}\right)^2}{1 - \left(\frac{\omega}{\omega_c}\right)^2} \qquad 9.12$$

This equation is plotted in Figure 9.6. This figure is seen to be similar to Figure 19a of Technical Report No. 1.

Since the assumption $\partial/\partial\theta = 0$ was made in order to arrive at Equation 9.12, this relation is not applicable to the case of the multi-anode magnetron.

A similar analysis for the cases of radial propagation with $\partial/\partial\vartheta \neq 0$ and the case of propagation in the ϑ direction is being carried out.

B. Experimental investigation. In order to ascertain the validity of the results of the previous analytical treatment concerning the propagation of electromagnetic waves in a magnetron space charge, two experimental tubes are under construction. These are designed to duplicate as closely as possible the configuration of electric fields assumed in the preceding analysis. Both experimental tubes involve a resonant cavity within which will exist a rotating space charge with which the electromagnetic fields can interact. Measurements of the change in resonant wavelength and unloaded Q of the cavity will yield the desired information of effective dielectric constant and conductivity of the cloud.

In the above theoretical analysis no term has been included in the equations of motion to account for any energy loss by the electrons. This term will be included in future analysis. Also, the effective conductivity of the cloud can be determined by experiment.

1. Wave propagation in the direction of applied magnetic field. For this investigation, a half wave coaxial

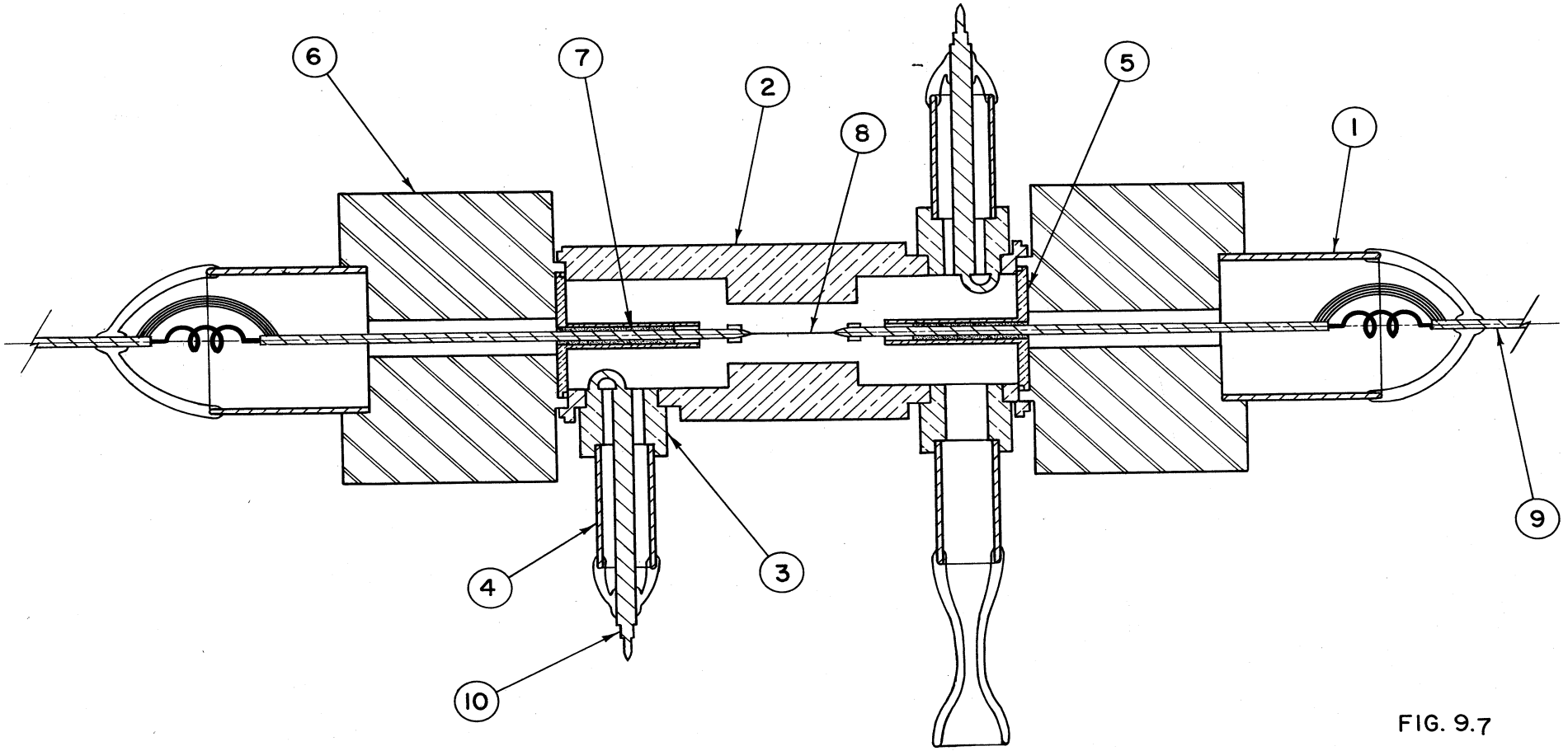

FIG. 9.7

ALL DIMENSIONS UNLESS OTHERWISE SPECIFIED MUST BE HELD TO A TOLERANCE - FRACTIONAL ± 1/64," DECIMAL ± .005," ANGULAR ± 1/2°

ENGINEERING RESEARCH INSTITUTE UNIVERSITY OF MICHIGAN ANN ARBOR MICHIGAN	DESIGNED BY GRB DRAWN BY ? CHECKED BY VRB
PROJECT M-762	TITLE 10 CM MAGNETRON DIODE (EXPERIMENTAL) MODEL 3
CLASSIFICATION	DWG. NO. B-11,003

ISSUE | DATE

APPROVED BY | SCALE | DATE 4-21-50

cavity has been constructed as shown in Figure 9.7. The central portion of the cavity was reduced in diameter in order to concentrate the r-f electric fields more in the region to be occupied by the space charge, and also to better confine the space charge in the desired region of the cavity. This tube has been made with two coupling loops to facilitate determination of the resonant wavelength; that is, this cavity can be used as a transmission circuit.

To date three tubes of this general design have been assembled; of these, two were lost in brazing, the third was completed and tested, but was made without the reduced diameter in the central portion of the cavity; as a result the space charge cloud was attracted by longitudinal components of d-c electric fields to the copper center conductor, making the formation of a cylindrical space charge cloud impossible. This defect has been corrected in the model shown in Figure 9.7. A tube of this design is now being assembled for test within a few days.

2. Wave propagation normal to the applied magnetic field. In order to make experimental observations of the space charge with r-f fields giving wave propagation in the radial direction ($E_\theta H_z$) the following arrangement is being considered.

The desired fields ($E_\theta H_z$) which have no circumferential variation can be obtained in a cylindrical cavity resonant in the TE_{01} mode. However, a cavity designed to

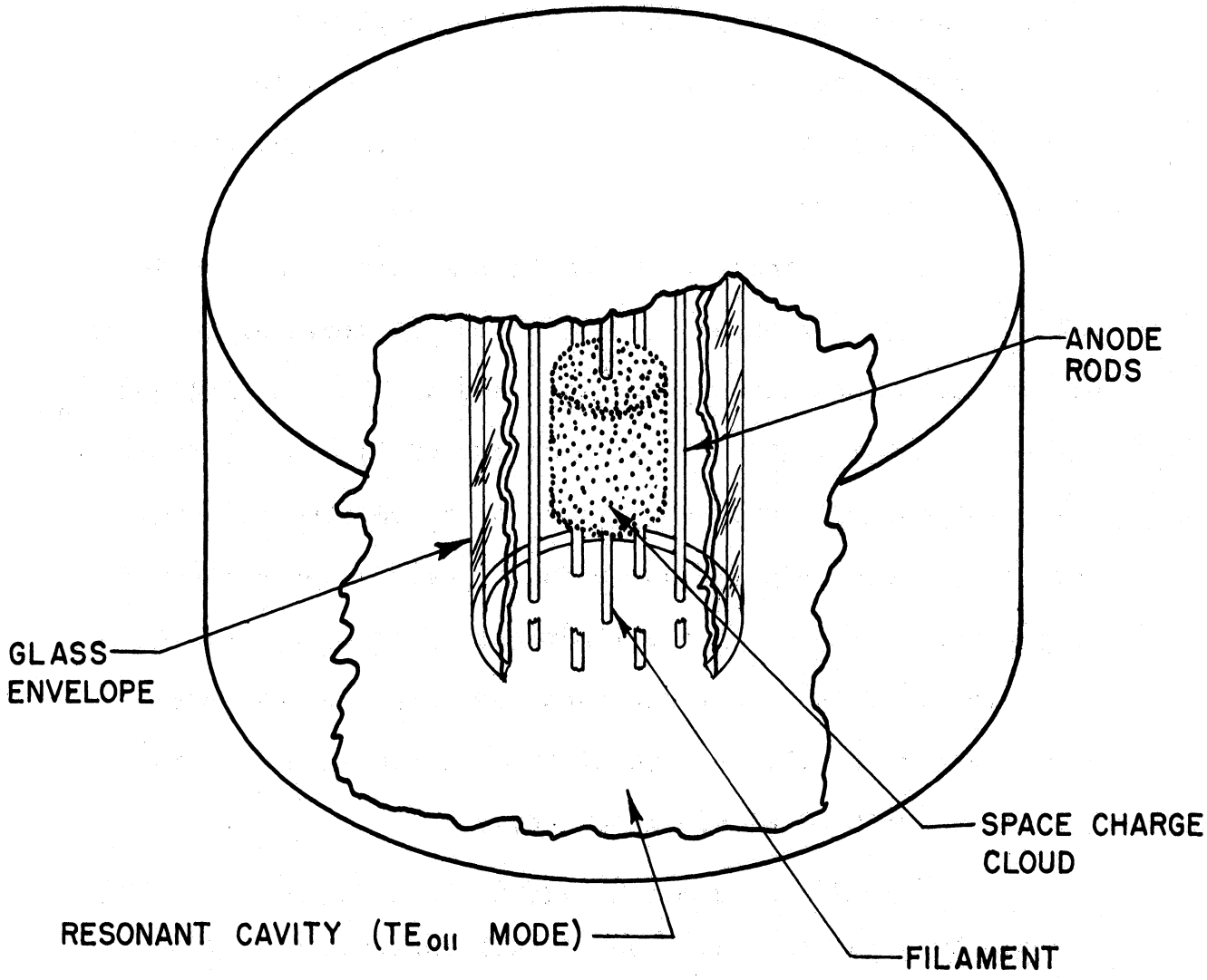

FIG. 9.8 TE_{011} RESONANT CAVITY FOR SPACE CHARGE STUDY

resonate at 10 centimeters in this mode will have a radius of approximately 7 centimeters, far too great to be used as the anode for the space charge. That is, for magnetic fields in the desired range (2000 gauss) an astronomical d-c voltage would be required to expand the space charge to a small fraction of this anode radius. Therefore it is proposed to use as the d-c anode a series of longitudinal rods spaced on a circle concentric with the cathode. If the rods are small enough and few in number, there will be relatively little metallic surface parallel to the θ directed electric field so that there should be only small perturbation of the r-f fields at the cathode. This arrangement is shown in Figure 9.8.

The question naturally arises as to the ability of such an anode to produce d-c equipotential lines which are approximately circles concentric with the cathode. A field map of a section of such a structure, made by Mr. J. S. Needle, is shown in Figure 9.9 from which it is seen that this anode approximates very closely a solid cyclindrical anode for any radius less than about 0.7 of the anode radius. This type of experimental tube has the advantage that only the longitudinal bars and the cathode need be included in the vacuum envelope; the cavity may be external to the vacuum.

A brass cavity suitable for this study has been constructed and preliminary tests made. The mode spectrum of such a cavity (7 centimeters radius, 7 centimeters long)

DWG. NO. A

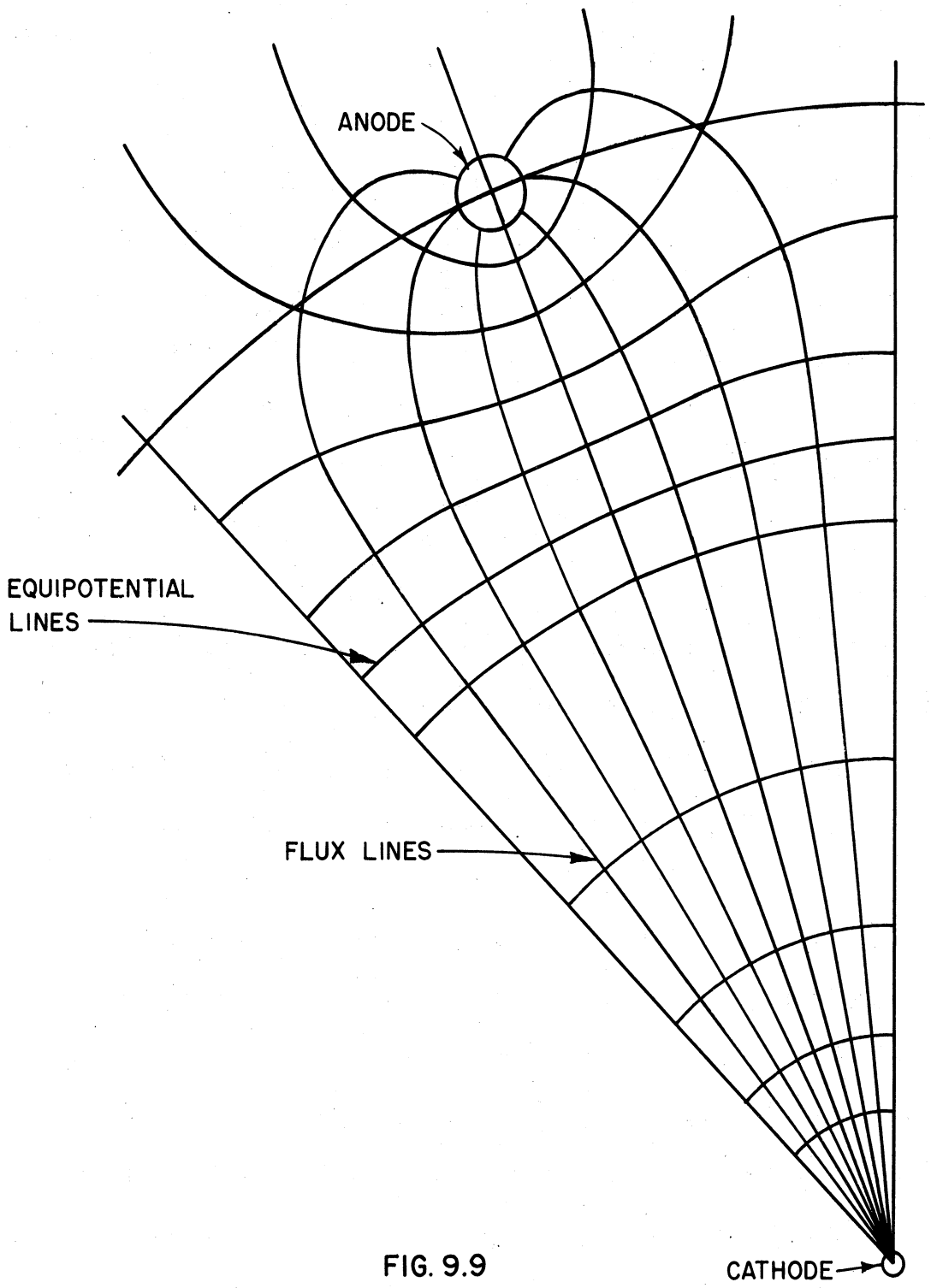

FIG. 9.9

ALL DIMENSIONS UNLESS OTHERWISE SPECIFIED MUST BE HELD TO A TOLERANCE - FRACTIONAL ± 1/64," DECIMAL ± .005," ANGULAR ± ½°

		ENGINEERING RESEARCH INSTITUTE UNIVERSITY OF MICHIGAN ANN ARBOR MICHIGAN	DESIGNED BY	APPROVED BY
			DRAWN BY MM	SCALE
			CHECKED BY	DATE 5-31 50
		PROJECT M-762	TITLE SECTION OF FIELD MAP OF CYLINDRICAL MAGNETRON	
ISSUE	DATE	CLASSIFICATION	DWG. NO. A-	

is naturally rather well filled, but the modes are identifiable. The insertion of a glass tube to simulate the vacuum envelope caused no appreciable shift in the resonant wavelength so that the electric fields are probably not distorted by this material.

10. CONSTRUCTION AND TESTING OF MAGNETRONS (J. R. Black, G. R. Brewer, H. W. Welch)

Two tubes have been emphasized during the period covered by this report. These are the Model 6 f-m tube (Figure 10.1) and the Model 7 coaxial magnetron (Figure 10.2). Data on Model 6 No. 26 was presented in the last Quarterly Report showing some promise in the modulating properties. However, the problem of losing power down the modulator cathode stem is still quite serious.

The Model 7 tube was built to be used in experimental work in the study of low Q operation. The first model does not have a low Q but is intended as a prototype for other tubes. Two outputs are provided, one coupled to the desired 14-centimeter mode and one to the undesired 9-centimeter mode. By selective loading, mode separation can be changed and some data on mode competition obtained.

The major emphasis of tube construction and testing during the period has been on the elimination of the cathode coupling problem in the Model 6 and Model 7 tubes. Better results than have been obtained could certainly be hoped for.

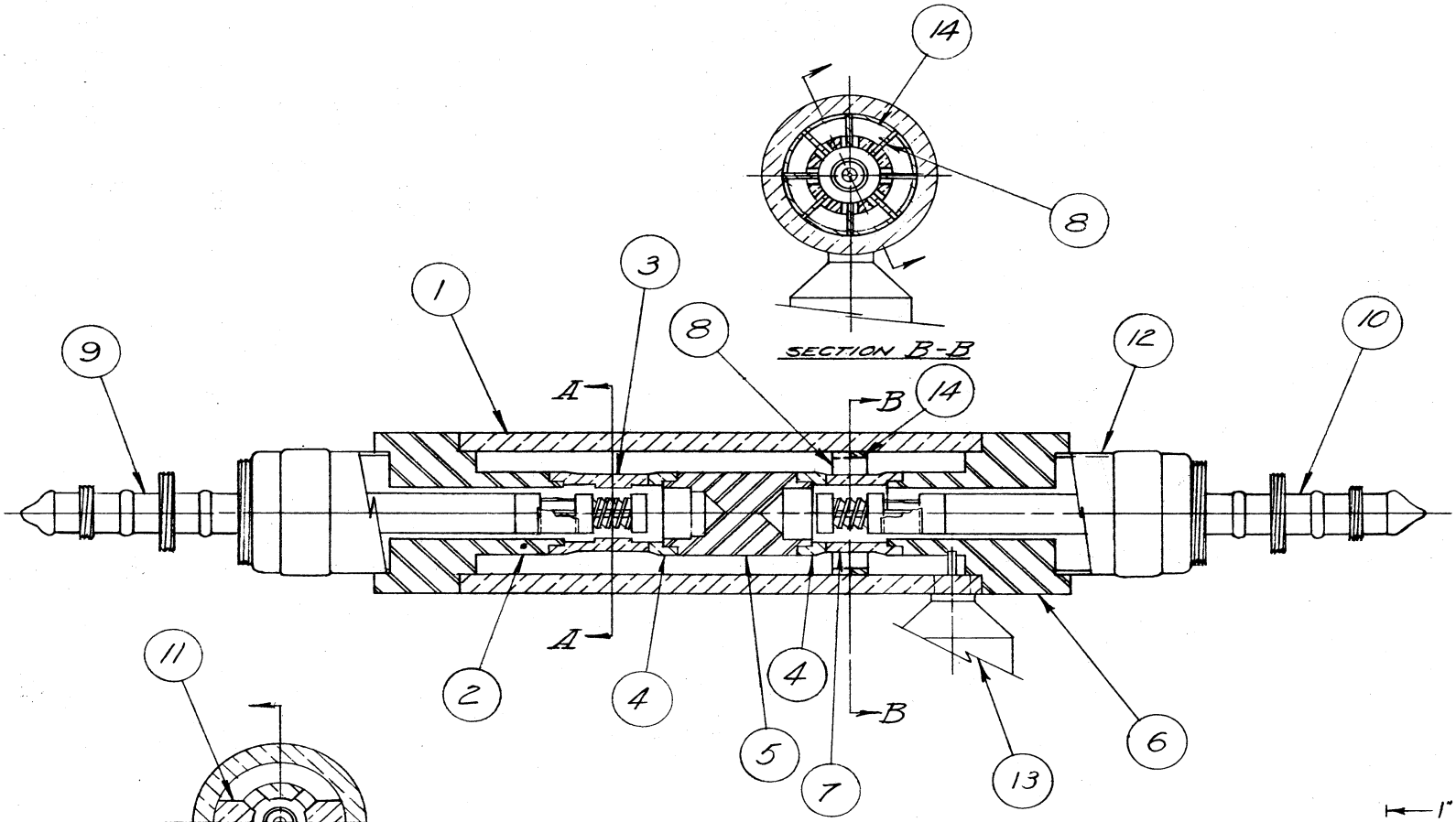

FIG. 10.1

ALL DIMENSIONS UNLESS OTHERWISE SPECIFIED MUST BE HELD TO A TOLERANCE - FRACTIONAL ± 1/64." DECIMAL ± .005." ANGULAR ± 1/2°

		ENGINEERING RESEARCH INSTITUTE UNIVERSITY OF MICHIGAN ANN ARBOR MICHIGAN	DESIGNED BY	APPROVED BY
			DRAWN BY JAN	SCALE FULL SIZE
			CHECKED BY VRB	DATE 2-20-50
		PROJECT M-762	TITLE FM MAGNETRON MODEL #6A	
1 ISSUE	2-20-50 DATE	CLASSIFICATION	DWG. NO. B-10,006A	

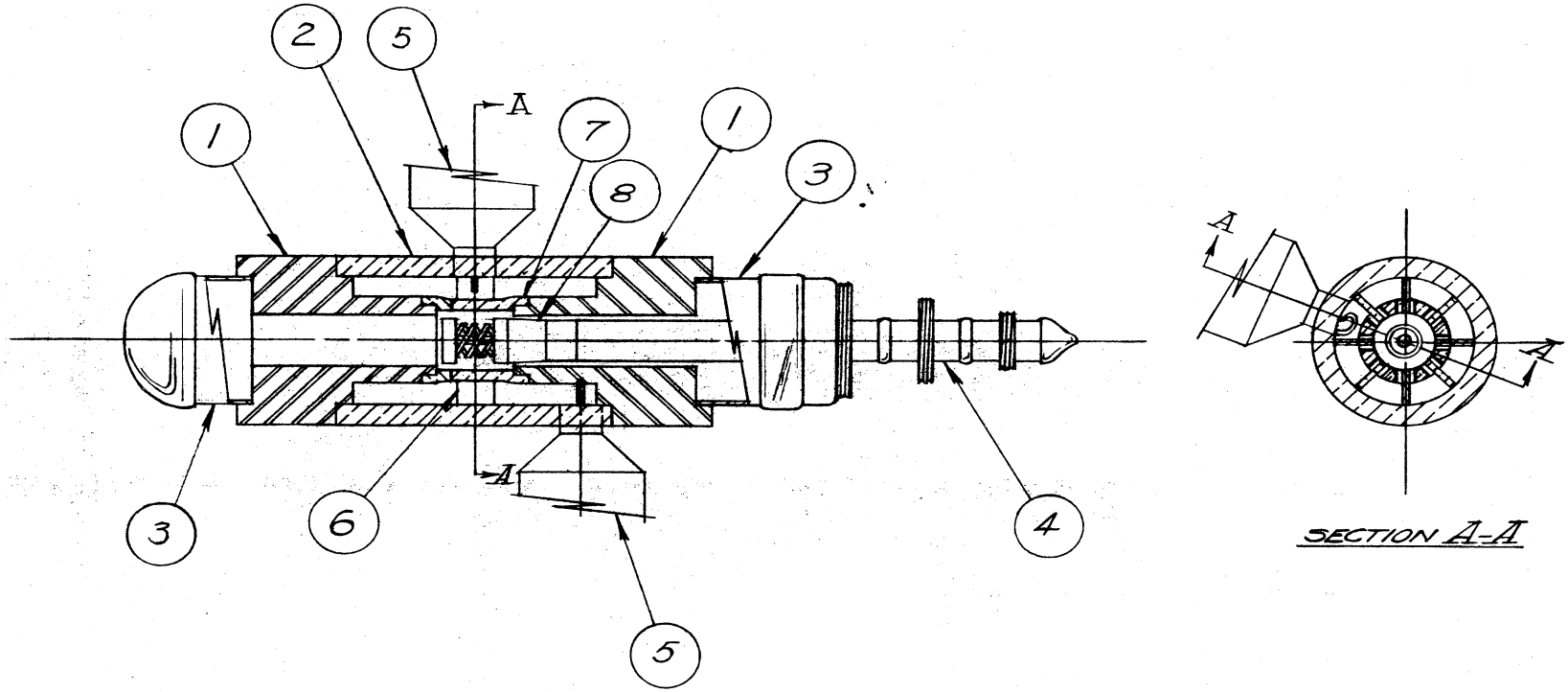

FIG. 10.2

ALL DIMENSIONS UNLESS OTHERWISE SPECIFIED MUST BE HELD TO A TOLERANCE - FRACTIONAL ± 1/64," DECIMAL ± .005," ANGULAR ± 1/2°

		ENGINEERING RESEARCH INSTITUTE UNIVERSITY OF MICHIGAN ANN ARBOR MICHIGAN	DESIGNED BY H.W.W	APPROVED BY
			DRAWN BY HW	SCALE FULL SIZE
			CHECKED BY JRB	DATE 12-2-49
		PROJECT M-762	TITLE CO-AXIAL MAGNETRON MODEL #7	
1	12/2/49	CLASSIFICATION	DWG. NO. B-10,007	
ISSUE	DATE			

The oscillator cathode has been improved to the point that both the Model 6 (see Figure 10.1) and the Model 7 (Figure 10.2) can be operated into a matched load. However, the Model 6 still will not operate satisfactorily with a modulator cathode in place. The history of the two models from the point of view of the cathode problem may be summarized as follows.

Model 6: Model 6A No. 31 was started in February. No. 31 differs from No. 26 in that a backing ring is provided in the vane section. This shortens the vanes and increases mode separation by changing resonant wavelength in the short wavelength mode from 10.96 to 9.2 centimeters. Modulation data which were obtained (see Figure 10.3) are almost identical with data obtained on Model 6 No. 26 (see last Quarterly Report). As before the tube had to be unloaded to obtain oscillation in the desired 13-centimeter mode. By shielding the cathode leads, it was discovered that more power was coupled out the leads than down the outside of the stem. It was decided to try an oxide-coated cathode where coupling to the leads would be impossible.

The modulator cathode was removed and the tube sealed up again without cathode. The oscillator performance results, which are encouraging, are shown in Figure 10.4. Power output of 190 watts was obtained at about 40 per cent efficiency. The oscillator cathode failed before more tests could be made.

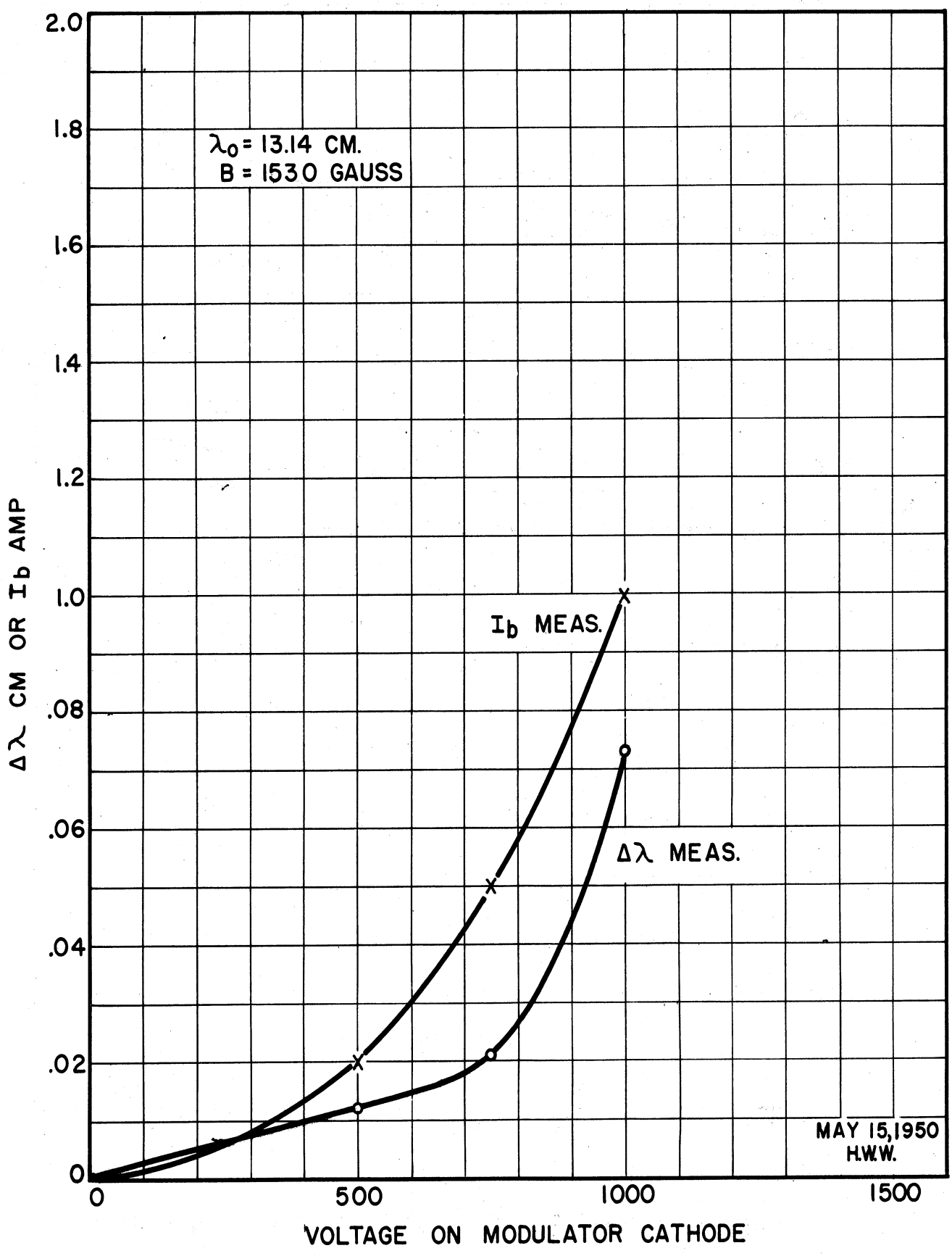

FIG. 10.3 MODULATION DATA ON MODEL 6 #31

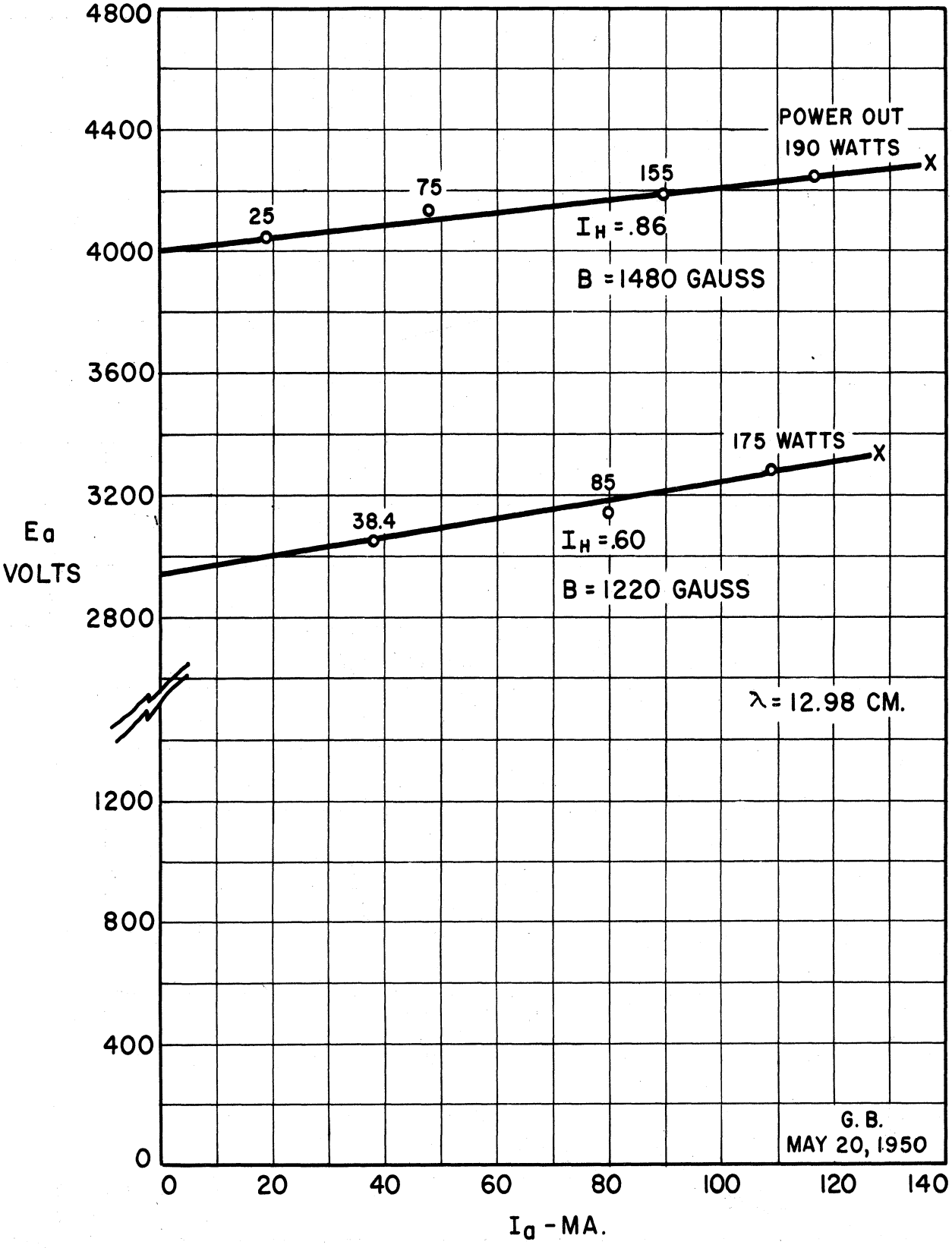

FIG. 10.4 PERFORMANCE DATA MODEL 6 NO. 31
WITHOUT MODULATOR CATHODE

Tests made after the modulator cathode was replaced with an oxide cathode showed power still coming out the outside of the cathode stem. New cathodes are currently being built which have enlarged stems to make the spacing in the cathode line as small as practical to increase the by-passing action.

The effect of adequate by-passing is shown in data taken on Model 7A No. 33. This tube also gave trouble with power leakage in the cathode although a previously built Model 7 was satisfactory. At first, coupling to the lead wires through the helix or pump-out holes in the cathode was suspected. Cold measurements showed this to be partially true but not as important as coupling outside the stem. The results of the Q measurements, made to determine the leakage and the effect of by-passing, are summarized below.

TABLE 10.1

Q Measurements on Model 7 No. 33

	Conditions	Q_o	Q_L	Q_{ext}
(1)	No cathode	1630	243	287
(2)	Standard cathode	338	200	490
(3)	Standard cathode with $\lambda/4$ copper by-pass	445	165	256
(4)	Same as (3) with helix shielded	977	208	265

It is assumed that the helix will not cause trouble when the tube is oscillating, since it will be surrounded by the swarm of electrons which sustain the oscillation. The tube has been rebuilt with a cathode having a $\lambda/4$ by-pass spaced as closely as possible to the anode. Operation was obtained into a matched load at 14 centimeters. However, an intermittent short between cathode and anode prevented the taking of extensive data.

In addition to the above-mentioned work on magnetrons: three magnetron diodes for experimental work on space charge problems have been built. Two of these were lost in processing. The third will be used in initial measurements for the program mentioned in section 8. Also, as was mentioned in section 7, parts for a low power magnetron are complete except for cathode. Work on the Model 5 f-m magnetron has been temporarily dropped. The Model 8 f-m magnetron (see last month's report) is completed except for cathodes.

11. CONCLUSIONS

Since all work in progress is in a state of partial completion, conclusions must be tentative. However, the progress during the period covered by this report may be summed up as follows:

(a) Results of the analysis of frequency pushing look favorable. In the present simple form of the analysis, the requirement of low Q circuits and of adjustment of

$Y_{oc}(\omega_o C)$ in proportion to Q for a given interaction space design is made evident. The next, probably more important, step is to find what interaction space can operate most favorably into low Q circuits.

(b) An overall understanding of the underlying causes of maximum current boundary has been reached. Analysis of more specific nature has been started and results may be expected in the near future.

(c) Design of a low power magnetron for low Q operation is well under way.

(d) A more complete analysis of the r-f properties of magnetron space charge has been made. This analysis shows possibility of amplification in the electron swarm. It also shows that the analysis presented previously (Technical Report No. 1) was a fair approximation in spite of restrictive conditions. The analysis will not be carried further in the near future. Experimental data for confirmation will be collected as soon as tubes and time are available.

(e) A program for static measurements and statistical analysis of distributions in the magnetron space charge has been started. The percentage of time devoted to this work is not very large; therefore, results are not to be expected in the very immediate future.

(f) The modulation of magnetrons by the reactance tube method has been held back by the problem of power leakage out the cathode of the modulator section of the tube. The

oscillator section has exhibited quite satisfactory performance.

12. WORK IN PROSPECT

The emphasis on study of low Q operation will be continued, with particular attention to cause of maximum current boundary and nature of temperature limited operation. Effort will be made to clean up the problem of power leakage to the cathode. At least one Model 8 magnetron will be completed. Work on Model 6 will continue. Experimental tubes for the study of low Q operation and space charge problems will be built.

DISTRIBUTION LIST

20 copies - Director, Evans Signal Laboratory
Belmar, New Jersey
FOR - Chief, Thermionics Branch

10 copies - Chief, Bureau of Ships
Navy Department
Washington 25, D. C.
ATTENTION: Code 930A

10 copies - Director, Air Materiel Command
Wright Field
Dayton, Ohio
ATTENTION: Electron Tube Section

10 copies - Chief, Engineering and Technical Service
Office of the Chief Signal Officer
Washington 25, D. C.

2 copies - H. Wm. Welch, Jr., Research Physicist
Electron Tube Laboratory
Engineering Research Institute
University of Michigan
Ann Arbor, Michigan

1 copy - Engineering Research Institute File
University of Michigan
Ann Arbor, Michigan

W. E. Quinsey, Asst to the Director
Engineering Research Institute
University of Michigan
Ann Arbor, Michigan

W. G. Dow, Professor
Dept. of Electrical Engineering
University of Michigan
Ann Arbor, Michigan

Gunnar Hok, Research Engineer
Engineering Research Institute
University of Michigan
Ann Arbor, Michigan

J. R. Black, Research Engineer
Engineering Research Institute
University of Michigan
Ann Arbor, Michigan

G. R. Brewer, Research Associate
Engineering Research Institute
University of Michigan
Ann Arbor, Michigan

J. S. Needle, Instructor
Dept. of Electrical Engineering
University of Michigan
Ann Arbor, Michigan

Dept. of Electrical Engineering
University of Minnesota
Minneapolis, Minnesota
ATTENTION: Prof. W. G. Shepherd

Westinghouse Engineering Laboratories
Bloomfield, New Jersey
ATTENTION: Dr. J. H. Findlay

Columbia Radiation Laboratory
Columbia University Dept. of Physics
New York 27, New York

Electron Tube Laboratory
Dept. of Electrical Engineering
University of Illinois
Urbana, Illinois

Dept. of Electrical Engineering
Stanford University
Stanford, California
ATTENTION: Dr. Karl Spangenberg

National Bureau of Standards Library
Room 203, Northwest Building
Washington 25, D. C.

Radio Corporation of America
RCA Laboratories Division
Princeton, New Jersey
ATTENTION: Mr. J. S. Donal, Jr.

Dept. of Electrical Engineering
The Pennsylvania State College
State College, Pennsylvania
ATTENTION: Prof. A. H. Waynick

Document Office - Room 20B-221
Research Laboratory of Electronics
Massachusetts Institute of Technology
Cambridge 39, Massachusetts
ATTENTION: John H. Hewitt

Bell Telephone Laboratories
Murray Hill, New Jersey
ATTENTION: S. Millman

Special Development Group
Lancaster Engineering Section
Radio Corporation of America
RCA Victor Division
Lancaster, Pennsylvania
ATTENTION: Hans K. Jenny

Magnetron Development Laboratory
Power Tube Division
Raytheon Manufacturing Company
Waltham 54, Massachusetts
ATTENTION: Edward C. Dench

Vacuum Tube Department
Federal Telecommunication Labs, Inc.
500 Washington Avenue
Nutley 10, New Jersey
ATTENTION: A. K. Wing, Jr.

Microwave Research Laboratory
University of California
Berkeley, California
ATTENTION: Prof. L. C. Marshall

General Electric Research Laboratory
Schenectady, New York
ATTENTION: Dr. Wilbur Hull

Cruft Laboratory
Harvard University
Cambridge, Massachusetts
ATTENTION: Prof. E. L. Chaffee

Research Laboratory of Electronics
Massachusetts Institute of Technology
Cambridge, Massachusetts
ATTENTION: Prof. S. T. Martin

Collins Radio Company
Cedar Rapids, Iowa
ATTENTION: Robert M. Mitchell

Dept. of Electrical Engineering
University of Kentucky
Lexington, Kentucky
ATTENTION: Prof. H. Alex Romanowitz

Dept. of Electrical Engineering
Yale University
New Haven, Connecticut
ATTENTION: Dr. H. J. Reich

Department of Physics
Cornell University
Ithaca, New York
ATTENTION: Dr. L. P. Smith

Document Office for Government Research Contracts
Harvard University
Cambridge, Massachusetts
ATTENTION: Mrs. Marjories L. Cox